Zn isotope fractionation during uptake into marine phytoplankton: Implications for oceanic zinc isotopes

Author(s):
Köbberich, Michael; Vance, Derek

Publication date:
2019-09-30

Permanent link:
https://doi.org/10.3929/ethz-b-000366870

Originally published in:
Chemical Geology 523(S), https://doi.org/10.1016/j.chemgeo.2019.04.004

Funding acknowledgement:
143262 - The development and application of transition metal isotope systems in surface Earth geochemistry (SNF)

Zn isotope fractionation during uptake into marine phytoplankton: implications for oceanic zinc isotopes

Michael Köbberich[1*] and Derek Vance[1]

*To whom correspondence should be addressed

Submitted to: ***Chemical Geology***

Special issue: ***GEOTRACES - Goldschmidt Session 10i***

Corresponding author

Michael Köbberich, phone: +41 (0) 44 632 07 30, email: michael.koebberich@alumni.ethz.ch

Author affiliations

[1] Institute of Geochemistry and Petrology, Department of Earth Sciences, ETH Zurich, Clausiusstrasse 25, CH-8092 Zurich, Switzerland

Running head

Ligand controlled Zn isotope fractionation

Keywords

Zinc isotopes, Ligands, Phytoplankton culturing, Metal uptake, GEOTRACES, Trace Metals.

Abstract

The extreme scarcity of zinc (Zn) in the euphotic zone, coupled to deep enrichments, is consistent with biological uptake at the surface and regeneration at depth. In the context of a nutrient-type depth profile so clearly shaped by uptake into phytoplankton, the growing dataset for Zn isotopes presents a challenge. These data either show very minor isotope effects associated with extreme depletion, or enrichment of the light isotopes in the upper ocean. In contrast, culturing of eukaryotes in the laboratory suggests that light Zn isotopes are preferentially taken up into diatoms and coccoliths, implying that Zn depletion at the surface should be associated with extremely heavy residual dissolved signals.

Here we present the first Zn isotope measurements for cultured marine cyanobacteria and compare these data to those for eukaryotic diatoms grown under identical conditions. Of the four cyanobacteria cultured, belonging to the genera *Synechococcus* and *Prochlorococcus*, three preferentially take up light Zn into the cell, with a variability that is not fundamentally different between pro- and eukaryotic phytoplankton. We also observe only very subtle differences between Zn/P and Fe/P uptake ratios for these three cyanobacteria groups relative to diatoms grown under the same conditions. A fourth strain exhibits preferential uptake of heavy Zn isotopes, and very high Zn/P ratios. Overall, we speculate that the observed variability among cyanobacteria may be related to the molecular structure of their photosynthetic light harvesting apparatus, adapted to significantly different light niches.

These new and published culture data support the hypothesis that cellular δ^{66}Zn in culture might largely be controlled by the organic ligands that bind Zn in the medium. Given that the Zn-binding ligands in the ocean have thermodynamic stability constants that are orders of magnitude smaller than the EDTA used in culture media, the surprisingly subtle Zn isotope variability in some parts of the surface ocean may be reconciled with culture data by the lesser, near zero, preference of these weaker complexes for heavy Zn isotopes.

1. Introduction

Intracellular metal quotas (Twining and Baines, 2013; Twining et al., 2003) show that zinc (Zn) and iron (Fe) are the two most abundant trace metals in marine phytoplankton (Morel et al., 2014; Twining and Baines, 2013). Extremely low bioavailable Fe concentrations limit the fixation of atmospheric carbon dioxide (CO_2) by phytoplankton in about 30% of the global surface ocean (Moore et al., 2013), and likely also near the deep chlorophyll maximum of stratified subtropical mid-ocean gyres (Hopkinson and Barbeau, 2008; Sedwick et al., 2005; Sunda and Huntsman, 2015). Although the jury is still out on whether Zn co-limits phytoplankton growth in certain regions of the global ocean (*c.f.* Moore et al., 2013), Zn is often equally, if not more, abundant in the cell than Fe (Twining and Baines, 2013). Both metals serve as co-factors in enzymes of key metabolic pathways. Important examples of Zn containing enzymes are carbonic anhydrases, essential during biomass buildup from reduced carbon (C) and light (Domsic et al., 2008; Morel et al., 2014; Roberts et al., 1997), or alkaline phosphatases for the acquisition of organic phosphorus (P) when phosphate is scarce (Cox and Saito, 2013; Morel et al., 2014; Shaked et al., 2006). Superoxide dismutases can also require sizeable fractions of the cellular Fe and Zn pool, in particular in phototrophs, where light-induced reactions often come with toxic superoxide anions (O_2^-) that can be reduced by this enzyme (Morel, 2008; Wolfe-Simon et al., 2005). As a result, Zn is extremely scarce in the surface ocean, while the deep ocean is enriched, consistent with biological uptake in the euphotic zone and its regeneration at depth (Bruland, 1980; Bruland et al., 2014).

Metal stable isotope data, increasingly available through the international GEOTRACES program, provide a new way of investigating the impact of trace metal availability on phytoplankton growth. However, the data available to date for oceanic Zn isotopes have presented some challenging puzzles. For example, despite drawdown by diatom uptake during northward flow of surface waters, of close to 99% of the Zn upwelled in the Southern Ocean, the Zn-depleted residual water is not shifted to very heavy values (Wang et al., this volume; Zhao et al., 2014), as would be expected for preferential uptake of light isotopes into cells.

Furthermore, for nearly all regions outside the Southern Ocean (Conway and John, 2014; Conway and John, 2015; John et al., 2018), dissolved Zn in the upper ocean is significantly enriched in light Zn isotopes compared to the globally rather homogeneous deep ocean. Though Samanta et al. (2017) invoke the uptake of light isotopes with decreased Zn abundances in the surface Tasman Sea, the data are noisy, the correlation is very weak (r^2 = 0.21, MSWD = 15) and the fractionation factor implied is within uncertainty of zero. The same very weak relationship and near zero fractionation are seen in the data of Wang et al. (this volume). These findings seem to be at odds with the expectation that light isotopes would be preferentially taken up into cells, and with laboratory culture experiments that find the biomass of marine eukaryotic algae to be enriched in light Zn isotopes with respect to the experimental medium (John and Conway, 2014; John et al., 2007; Köbberich and Vance, 2017; Köbberich and Vance, 2018; Samanta et al., 2017).

Taxonomic differences among distinct groups of phytoplankton have been considered to drive some of the observed regional and global variability in Zn abundances in the ocean. For example, elevated Zn in diatoms (Twining and Baines, 2013) has been suggested to control Southern Ocean concentrations and, through the water masses advected from it, the pattern of variability in the global ocean (Vance et al., 2017). On the other hand, it is well-established that cellular Zn is closely related to its bioavailability in seawater (Sunda and Huntsman, 1992), leaving it unclear to what extent changes in the proteome are relevant (Cox and Saito, 2013; Twining and Baines, 2013). Beyond diatoms, Samanta et al. (2017) observed electron transport rates and the photosynthetic efficiency to increase with increasing free Zn^{2+} concentration in another eukaryote, *Emiliania huxleyi*, which was speculated to be due to increased carbonic anhydrase activity.

The global biogeography of phytoplankton is such that a great deal of the total chlorophyll belongs to only two major groups of phytoplankton, namely *Synechococcus* or *Prochlorococcus* (Follows and Dutkiewicz, 2010; Follows et al., 2007; Menemenlis et al., 2005). Furthermore, these prokaryotic cyanobacteria are direct descendants of the earliest

oxygenic phototrophs, originating during a period of Earth history distinctly different in its ocean chemistry (Falkowski and Knoll, 2007; Knoll et al., 2012; Saito et al., 2003; Sunda and Huntsman, 2015). It has been suggested that this resulted in elevated minimum Fe requirements in prokaryotes, and that this explains their high requirement for Fe relative to eukaryotes in the modern ocean (Brand, 1991; Österberg, 1974; Saito et al., 2003; Sunda and Huntsman, 2015).

In the light of these considerations, constraints on how cyanobacteria take up Zn and its isotopes are required. Here we address this requirement. We also present new data for diatoms, cultured under conditions that are as close as possible to those for the cyanobacteria. Our aim is to explore the relative importance of species-dependent differences versus environmental controls for trace metal systematics versus, with implications for the evolution of trace metal requirements in an ocean in which the biology and chemistry have both changed through time. Finally, we consider the emerging dataset for oceanic Zn isotopes in the context of these new constraints, as well as published data, from culture experiments.

2. Materials & Methods

Culturing media were prepared either from salts that were of trace metal purity, or from solutions that were cleaned using a chelating resin (Chelex® 100, Bio-Rad, USA). All ultrapure water came from a Milli-Q® integral water purification system (Merck, Millipore, Germany) with a conductivity of 18.2 MΩ·cm. Reagent grade acids used for preparative purposes were twice purified by sub-boiling distillation before use (DST-1000, Savillex, USA). Handling of all samples and reagents was carried out under "Class 100" clean laboratory conditions at constant humidity of around 10 %, and a temperature of 21.2 ± 0.2 °C.

2.1 Phytoplankton strains

Three different diatoms and four distinct cyanobacteria strains, all axenic, were obtained from the National Center for Marine Algae and Microbiota (NCMA), formerly known as Provasoli-Guillard Center for Culture of Marine Phytoplankton (CCMP), Bigelow Laboratories, USA.

Two of the chosen diatoms, *Chaetoceros sp.* (CCMP 199) and *Thalassiosira oceanica* (CCMP 1005), originate from oligotrophic surface waters of the Sargasso Sea, North Atlantic. The third, *Thalassiosira weissflogii* (CCMP 1336) came from coastal waters of Long Island Sound, North Atlantic, USA. Three representatives of the genus *Synechococcus* (CCMP 1183, 1334, and 2370, the latter two are also known as WH 7803 and 8102) and *Prochlorococcus marinus* (CCMP 2389, *a.k.a.* MED 4) were chosen to represent the prokaryotic phylum of cyanobacteria. All four prokaryotes are open ocean strains, two of which (CCMP 1334 and 2370) originate in the oligotrophic surface waters of the Sargasso Sea, North Atlantic. Sterile techniques were used whenever cultures or media solutions were handled. Axenic conditions were monitored by inspecting small aliquots of stained culture solutions by microscopic methods.

An important aim of this contribution is to explore inter-species Zn isotope effects associated with Zn uptake into the cell. Biological fractionation of Zn isotopes during uptake has been related to active transport across the cell membrane (John et al., 2007), a mechanism that for Fe has been shown to be a surface-area related process (Sunda and Huntsman, 1995; Sunda and Huntsman, 1997). The set of species chosen here span the entire size range of pico- and nano-phytoplankton and differ in their surface area to biovolume (A/V) ratio as calculated from their cellular geometry (Fig. 1). The cellular dimensions and geometries of 1362 diatoms (Leblanc et al., 2012) and 181 coccolithophores (O'Brien et al., 2013) came from the MARine Ecosystem DATa (MAREDAT; Buitenhuis et al., 2013) project. Geometric models that are used for calculating cell surface areas and biovolumes (Leblanc et al., 2012; Sun and Liu, 2003) can also be linked to empirical carbon (C) biomass estimates (Leblanc et al., 2012; Smayda, 1978). We use this information to compare our laboratory cultures with the A/V ratios that have previously been considered relevant to natural environments (Fig. 1).

2.2 Culturing techniques

The culturing conditions were similar to Köbberich and Vance (2017). A short summary is given below with the most important differences highlighted. Light was supplied to all

phytoplankton cultures in 15- to 9-hour day to night cycles. A constant photon flux density of 50 rather than 40 μmol m^{-2} s^{-1} was used, with one important exception: the high light adapted *Prochlorococcus* strain CCMP 2389 was maintained at 25 μmol m^{-2} s^{-1}, as verified with a newly calibrated spherical quantum sensor LI-193 (LI-COR®, Nebraska, USA). Cell numbers for calculating specific growth rates were obtained by Coulter counting on a daily basis or by using a hemocytometer, as described in Köbberich and Vance (2017).

The artificial culture medium, used here to allow comparison across a range of different eukaryotic and prokaryotic phytoplankton organisms at similar bioavailable Zn^{2+} levels, is similar to that previously reported in Köbberich and Vance (2017). This medium has a seawater base adjusted to a final salinity of about 36 g kg^{-1}. Total ethylenediaminetetraacetic acid (EDTA) concentrations were in the range 95 - 97 μmol l^{-1}, and Zn was kept constant to allow inter-species comparison at identical bioavailable Zn. Total Zn concentrations were thus adjusted to obtain free divalent Zn^{2+} and inorganically bound Zn (Zn′) levels in the range 67 - 72 and 100 - 109 pmol l^{-1}, respectively, for all eukaryotes and *Synechococcus* strains. Aqueous Zn speciation has been calculated following the recommendations of Sunda et al. (2005) and references therein. The artificial seawater medium used to culture the *Prochlorococcus* strain CCMP 2389 had to differ from that used for all other strains for two distinct, though related, reasons. Firstly, *P. marinus* simply does not grow in the above-described broad-spectrum medium. Secondly, to our knowledge, there is currently no recipe available that maintains *Prochlorococcus* as well as all the other species of interest. We thus designed a newly developed medium that mimics the above-described solution as closely as possible, while still achieving sufficient *Prochlorococcus* growth (see Supplementary Information S.1 for further details).

All phytoplankton cells were harvested, *i.e.* separated from their residual culturing medium, at or shortly after mid exponential growth, with 0.2 μm filters, using pre-cleaned vertical twin membrane centrifugal concentrators (Vivaspin 20, Sartorius, Germany). Shortly after harvesting, residual media remnants were removed by washing the collected cells with UV-

178 treated equatorial Atlantic seawater, with notably low Zn in the range of 0.01 - 0.05 nmol kg^{-1}
179 (Zhao, 2011). The biomass collected on the filter was re-suspended in pre-cleaned NaCl of
180 seawater osmolality, before the resulting cell suspension was pipetted out of the centrifugal
181 concentrator. After evaporation to dryness, all samples were digested in double distilled 65%
182 HNO_3 at 120 °C for ~16 hours. After a final dry-down, all digested samples were re-dissolved
183 in 2 % HNO_3 for elemental analysis, followed by column chromatography and Zn isotopic
184 analysis (see next section).

185 **2.3 Elemental and stable isotope analysis**

186 The procedures used for elemental and stable isotope analysis are identical to those previously
187 described in Köbberich and Vance (2017) and very similar to those in previous publications
188 from this laboratory (*e.g.*, Little et al., 2016; Vance et al., 2016a; Vance et al., 2016b). In brief,
189 elemental analyses were done on a ThermoScientific Element XR™ inductively-coupled
190 plasma mass spectrometer (ICP-MS). All samples for isotope analysis were purified by anion
191 exchange chromatography (Archer and Vance, 2004; Bermin et al., 2006; Maréchal et al.,
192 1999) and were measured on a Neptune Plus™ multiple-collector inductively-coupled plasma
193 mass spectrometer (MC-ICP-MS) of the same manufacturer. Instrumental mass fractionation,
194 or that occurring during ion exchange chromatography, was corrected using the double spike
195 approach as described by Bermin et al. (2006) and Zhao et al. (2014), in combination with a
196 data reduction scheme presented by Siebert et al. (2001). Procedural blanks were estimated by
197 isotope dilution analysis and are negligible.

198 The data presented here are given in the standard delta notation, in per mil, reported relative to
199 JMC 3-0749 (Maréchal et al., 1999): $\delta^{66}Zn$ (‰) = $[(^{66}Zn/^{64}Zn)_{sample} / (^{66}Zn/^{64}Zn)_{JMC\text{-}Lyon}] - 1$.
200 Accuracy and precision were monitored relative to a secondary standard, IRMM-3702,
201 previously reported to yield a value of +0.32 ‰ (Cloquet et al., 2008; Ponzevera et al., 2006).
202 Relative to JMC-Lyon, we obtain $\delta^{66}Zn = 0.30 \pm 0.06$ ‰ (2 SD, n = 163 over 380 days). All
203 our culturing results are reported as the fractionation observed between the medium and the
204 separated biomass, here denoted $\Delta^{66}Zn$ (‰) = $\delta^{66}Zn_{biomass} - \delta^{66}Zn_{medium}$. Culture experiments

were only considered relevant for reporting when nearly 100% of the Zn initially added to the medium was recovered in the residual medium plus the biomass fraction after the experiment, as quantified by isotope dilution. All diagrams plot the external precision, based on replicate analyses of IRMM-3702 as noted above, unless internal errors exceed the external reproducibility.

3. Results

Based on measured growth and metal uptake data, the largest cultured diatom, *T. weissfloggi*, reached Zn uptake rates up to about 26% of the maximum that could be supplied to the cell by diffusion (Table 1). The prokaryotic organisms cultured here were much less likely to be diffusion limited - and consistently contained less than 1% of the amount of Zn that could be supplied by diffusion. Fe exerts a key control on phytoplankton growth and thus metal uptake (Köbberich and Vance, 2017; Sunda and Huntsman, 1995; Sunda and Huntsman, 1997), so that Table 1 also provides data supporting the suggestion that growth it not suppressed as a consequence of diffusion limited Fe supply.

Three different diatom strains, each grown on nitrate and urea as the sole N source, were generally found to grow fast, with specific growth rates between 0.65 and 0.77 d^{-1}. At identical irradiance and nutrient levels, three representatives of the genus *Synechococcus* grew at more variable rates, ranging from 0.42 to 0.82 d^{-1} (Fig. 2A). *Prochlorococcus marinus* – the smallest strain cultured here – grew at a specific growth rate of 0.28 d^{-1}, at half the irradiance level (25 μmol m^{-2} s^{-1}) applied to all other strains (50 μmol m^{-2} s^{-1}).

Fe uptake into marine phytoplankton has previously been shown to be a surface area related process (Sunda and Huntsman, 1995; Sunda and Huntsman, 1997). Surface area normalized Fe and Zn uptake rates, calculated from measured cellular quotas and the surface areas shown in Fig. 1, are high and variable for diatoms, reaching up to values that are often greater than 100 nmol m^{-2} d^{-1}. Those of prokaryotes are mostly much lower (Fig. 2B and C).

Carbon or P-normalized cellular Fe and Zn of all measured diatoms are in good agreement with previous culture work (Sunda and Huntsman, 1992; Sunda and Huntsman, 1995) at similar bioavailable metal concentrations. Measured metal to P quotas were converted to Zn/C assuming a Redfield stoichiometry of C:P of 106:1. In good agreement with previous work on a coastal *Synechococcus bacillaris* strain (Sunda and Huntsman, 2015), all studied cyanobacteria yielded higher cellular Fe quotas than the majority of cultured diatoms (Fig. 3A), while their absolute rates of metal transport across the cell membrane were generally found to be very low (Fig. 2B). Except for the *Synechococcus* strain CCMP 2370, the opposite was found for cellular Zn quotas (Fig. 3B), also at comparatively low uptake rates (Fig. 2C). This becomes most apparent if cellular Zn quotas are plotted as a function of Fe quotas (Fig. 3C). Excluding CCMP 2370, the highest Zn/P quotas of ~2 mmol mol^{-1} were found with low Fe/P ratios, while the lowest of ~0.5 mmol mol^{-1} were reached at Fe/P ~7 mmol mol^{-1}.

All the isotope results are given in Table 1. The biomass of the marine diatom *T. oceanica* shows a preference for light isotopes by 0.28‰, similar that previously observed for this strain for a comparable culture medium (Δ^{66}Zn; John et al., 2007; Köbberich and Vance, 2017).

4. Discussion

Of the two groups of organisms cultured here for Zn isotopes, the data for cyanobacteria are the most novel. Previous studies have presented data for diatoms (John et al., 2007; Köbberich and Vance, 2017; Köbberich and Vance, 2018), while Samanta et al. (2017) have published Zn isotope data for another eukaryote group, the coccoliths. Thus, we first discuss the variation within the cyanobacteria strains cultured, before moving on to compare these new data with the new and published data for eukaryotes.

4.1 Variations in metal uptake characteristics among cyanobacteria

Three of the four cyanobacteria cultured were found to have similar cellular Zn quotas to diatoms, though at the lower end of the latter's range. The opposite is true for cellular Fe quotas (Fig. 3A and 3B), a finding which is in agreement with previous work (Saito et al., 2003; Sunda

and Huntsman, 2015; Sunda and Huntsman, 1995). It is also obvious from Fig. 3, that CCMP 2370 differs from the other cyanobacteria in its Zn quota. Though this difference is less marked for Fe, it is also the case that the Fe quotas found for CCMP 2370 represent the higher end of the observed spectrum (Fig. 3C). High biomass associated Fe contents might indicate the presence of surface-bound Fe-hydroxides, which could adsorb large quantities of Zn, and this theory might be supported by positive biomass Δ^{66}Zn values (see Table 1 and Section 4.3; Gélabert et al., 2006; John et al., 2007). However, the variability in the overall cyanobacterial dataset, for both Fe- and Zn-quotas and including the data for CCMP 2370, is no greater than that seen in natural communities using X-ray fluorescence imaging techniques (Twining and Baines, 2013). Moreover, Tang and Morel (2006) did not detect any increase in cellular Zn/P at the total medium Fe concentrations used here, or for the biomass Fe/P ratios measured here. It is also the case that CCMP 2370 differs from all other cyanobacteria in the greater proportion of phycourobilin (PUB) in its total budget of chromophores (Six et al., 2007). There is, however, currently no known Zn containing enzyme involved in the biosynthesis of PUB. Whether the cellular Zn content could be related to such biochemical pathways remains to be addressed in future research (for additional thoughts see section S.5 of the Supplementary Information).

4.2 Similarities and differences between prokaryotic and eukaryotic metal uptake

Culture experiments are performed in a controlled environment. An assessment of taxonomic differences from such experiments is often only possible in terms of whether the phytoplankton of interest is well adapted to the culture conditions used, coupled to a comparison between those culturing conditions and the organism's natural habitat. Thus, despite an extensive body of literature on the physiological response to various types of environmental stress (for a review see Morel et al., 2014) applied in laboratory cultures, it remains challenging to separate purely taxonomic effects from imposed environmental factors.

The precise culture conditions chosen here for the eukaryotic organisms were adjusted to yield similar specific growth rates for each organism, using published constraints (Sunda and

Huntsman, 1995; Sunda and Huntsman, 1997). Thus, though the open ocean diatom *T. oceanica*, as well as a representative of the genus *Chaetoceros*, grew at similar rates for the same Fe′, the same growth rates were only achieved for the coastal species, *T. weissflogii*, at Fe′ that was almost twice as high (Table 1). Prokaryotes such as the tiny *Prochlorococcus* simply behave too differently to reasonably expect them to yield the same fast growth rates as diatoms in culture (*c.f.* Supplementary Information S.1). In our experiments, CCMP 1183 and 2370 were at least close, though somewhat more variable (Fig. 2A).

4.3 Ligand control on Δ^{66}Zn recorded in phytoplankton

Based on precautions to avoid diffusion-limited Zn transport towards the cell surface (*c.f.* section S.2 in the Supplementary Information), we can essentially exclude the possibility that any of the negative Δ^{66}Zn observed here are likely to be caused by the slightly faster diffusion rates of the lighter ^{64}Zn isotope. Only the cyanobacteria strain CCMP 2370, with unusually high cellular Zn quotas, was found to yield positive Δ^{66}Zn values with respect to the bulk culture medium (Fig. 4). All other phytoplankton, whether pro- or eukaryotic, consistently yielded negative Δ^{66}Zn values (Table 1). These findings are in good agreement with previous culture experiments (John et al., 2007; Köbberich and Vance, 2017; Samanta et al., 2017), at similar bioavailable Zn levels, as illustrated in Fig. 5.

The equilibrium fractionation between Zn-EDTA and 'free' Zn is such that heavy Zn isotopes are preferentially bound to the organic chelator (Ban et al., 2002; Ding et al., 2010a; Ding et al., 2010b; Markovic et al., 2017), while the bioavailable Zn^{2+} pool is enriched in light Zn isotopes - before any interaction with phytoplankton. In agreement with the suggestion of John et al. (2007), we thus argue that a substantial portion of the observed Δ^{66}Zn in cultured phytoplankton is actually the result of this equilibrium fractionation in the medium, rather than resulting from biological uptake. Although there is strain-dependent variability in the extent to which the light Zn isotope is taken up into phytoplankton, there are no systematic differences between cyanobacteria and diatoms. In fact, excluding CCMP 2370, the absolute ranges observed among different representatives of both clades are almost indistinguishable from each

other. Neither absolute rates of Zn transport across the cell surface area, nor A/V ratios (see Supplementary Information, Fig. S.1), seem to correlate with the extent to which light Zn isotopes are preferentially taken up. This could simply be due to the fact that the studied diversity is still too small, obscuring any potential pattern. On the other hand, the uptake mechanism may be important, given that there is an increasing preference for light Zn isotopes as a result of additional active transport across the cell wall beyond the level associated with high-affinity transporters alone (John et al., 2007). Thus, the observed variability might be caused by the fact that the onset of low-affinity Zn uptake may occur at different bioavailable Zn concentrations, as previously identified for *T. oceanica* (John et al., 2007) and *Emiliania huxleyi* (Samanta et al., 2017). In this study, bioavailable Zn was chosen to be at the higher end of the range previously considered relevant for high-affinity uptake (for a more detailed discussion, see Köbberich and Vance, 2017). Thus, it is possible that light signatures seen in some of the strains studied here might be explained by isotope fractionation associated with active low-affinity transporters superimposed on a fractionation caused by the high-affinity mechanism.

5. Conclusion and oceanic implications

The two first order features of the oceanic distributions of Zn isotopes that are emerging as data accumulates are: 1) in the Southern Ocean, despite often dramatic drawdown of Zn at the surface, mostly by diatoms, variations in the small residual Zn pool are very muted (*e.g.*, Wang et al., this volume; Zhao et al., 2014); 2) outside the Southern Ocean, residual seawater tends to be lighter in the upper ocean, seeming to imply the uptake of heavy isotopes (*e.g.*, Conway and John, 2014), though where high depth resolution is available near the surface it is often the case that these light values actually occur in the immediate sub-surface (*e.g.*, Wang et al., this volume). Though variations in dissolved Zn isotopes in the surface Southern Ocean are indeed muted, there is also a slight minimum at 100-200m (Wang et al., this volume). The above observations are both, at first glance, inconsistent with the finding of light Zn isotopes in

phytoplankton cells in culture. Here we discuss each of the above observations of the real ocean in turn, in the context of the summary of culturing experiments in Fig. 5.

An important conclusion from Fig. 5 is that a large proportion of the enrichment of light Zn in a variety of studied pro- and eukaryotic phytoplankton can be explained by the presence of organic ligands in culture media. Consistent with a postulate by John et al. (2007), heavy Zn isotopes are preferentially bound to the trace metal buffer EDTA in culture media, while the 'free' bioavailable Zn pool is already enriched in light isotopes before uptake. A significant proportion of light Zn found in phytoplankton after a culture experiment might thus be the result of an aqueous equilibrium in seawater, rather than the consequence of kinetic isotope fractionation during active transport across the cell wall. Although the uncertainty on the isotope fractionation associated with the relevant Zn-EDTA equilibrium is still large (Ban et al., 2002; Ding et al., 2010a; Ding et al., 2010b; Markovic et al., 2017), kinetic isotope effects associated with uptake are only rarely outside the range that could be explained by the presence of this strong ligand.

One could argue that, since the real ocean also contains strong ligands that bind Zn, it is still the Δ^{66}Zn fractionation with respect to bulk medium that is the most relevant for the great majority of oceanic regimes. For example, Ellwood and Van den Berg (2000) have shown that 94 - 99% of all Zn in the open NE Atlantic is bound to strong organic complexes. Free Zn concentrations - at 6 - 20 pmol l^{-1} - in those regions are low, but not low enough to limit the growth of a typical oceanic species (Ellwood and Van den Berg, 2000). Thus, the situation regarding complexation of Zn in the real ocean is *qualitatively* analogous to that in culture experiments, with the bioavailable pool being lighter than the ligand bound fraction.

In the surface Southern Ocean, Zn is rapidly drawn down by diatom uptake, by almost 2 orders of magnitude relative to the upwelled deep waters (*e.g.*, Vance et al., 2017; Zhao et al., 2014). If such uptake prefers the light isotope to the extent seen for $\Delta^{66}Zn_{\text{biomass - bulk medium}}$ in culturing experiments (Fig. 5), then the δ^{66}Zn of the residual Zn-depleted water should exceed 1‰, when in fact it barely rises above the deep ocean average δ^{66}Zn of +0.5‰ more than analytical

uncertainty (Wang et al., this volume; Zhao et al., 2014). ~~We suggest that the answer to this conundrum lies in the positive relationship, observed by Markovic et al. (2017) in experiment, between the degree of isotope separation between free Zn^{2+} and the organically-bound complex and the strength of that complex. Given that the conditional stability constants of Zn-binding by organic complexation in the real ocean are about 6 orders of magnitude lower than those for EDTA (*e.g.*, Ellwood and Van den Berg, 2000; Markovic et al., 2017), and given the relationship observed in Markovic et al. (2017), it may actually be no surprise that the real oceanic data often show more subtle isotope effects than cultures.~~ It could be that the answer to this problem originates with differences in the speciation of Zn in culture versus seawater. Markovic et al. (2017) present experimental findings showing that isotope fractionation between free Zn and the organically-bound complex depends on the thermodynamic stability constant for that complex, which for EDTA is about 6 orders of magnitude greater than those for Zn in the real ocean (*e.g.*, Bruland, 1989; Ellwood and van den Berg, 2000; Markovic et al., 2017). However, Bruland (1989) also showed that the *conditional* stability constant for Zn-EDTA complexes in seawater are lower than those for natural organic ligands, due to side reactions between EDTA and Ca and Mg ions that do not occur for the natural ligands (Bruland et al., 1989).

~~Finally, we turn to the apparently light Zn isotope values in areas outside the Southern Ocean, implying loss of *heavy* isotopes during Zn drawdown. John and Conway (2014) have suggested an explanation in terms of scavenging to particulate organic matter (John and Conway, 2014). One issue with this suggestion is that the experiment in which scavenging, and Zn isotope fractionation associated with it, was observed (John and Conway, 2014) contained none of the organic ligands that stabilize Zn in solution, whereas most of the surface ocean contains more than 10 times more Zn-specific ligands than total dissolved Zn found in the NE Atlantic (Ellwood and Van den Berg, 2000). The one part of the surface ocean where this is known not to be the case is the Southern Ocean, (Baars and Croot, 2011), and this is where heavy surface isotopes are not seen.~~

~~As shown in the data compilation in Wang et al. (this Volume), most profiles with generally negative δ^{66}Zn in the upper ocean actually feature a heavy value right at the surface. In at least some cases, this upward move to heavy Zn isotopes is defined by more than a single sample. We suggest, therefore, that there may, in fact, be uptake of slightly light isotopes at the surface and that the light isotopes that apparently dominate the upper ocean in *e.g.* the North Atlantic (Conway and John, 2014) are the result of very shallow sub-surface (peaking at about 100 m but extending down to 500 m) regeneration of biomass-associated light Zn isotopes (*e.g.*, Bermin et al., 2006). In this view, the data from the surface ocean is also not actually inconsistent with culture experiments that suggest slight preferential uptake of light isotopes into phytoplankton (Fig. 5). Such a hypothesis does require that Zn cycling up and down between the photic zone and the immediate sub-surface must, outside the Southern Ocean, be to a large extent decoupled from the deep ocean underneath. In this view, consistent with the behavior of other nutrients in the ocean, Zn behavior is split by a Southern Ocean biogeochemical divide (*e.g.*, Marinov et al., 2006; Sarmiento et al., 2004; Vance et al., 2017), with a Zn-rich deep cycle fed by deep waters from the Southern Ocean, and that only re-connects to the surface in the Southern Ocean, below a rather isolated extra-Southern shallow ocean that is fed by the Zn-poor upper ocean water masses advected out of the Southern Ocean.~~

Finally, we turn to the apparently light Zn isotope values in areas outside the Southern Ocean. John and Conway (2014) have suggested an explanation in terms of preferential loss of heavy isotope through scavenging to particulate organic matter. One issue with this suggestion is that the experiment in which scavenging, and Zn isotope fractionation associated with it, was observed (John and Conway, 2014) contained none of the organic ligands that stabilize Zn in solution, whereas most of the surface ocean contains more than 10 times more Zn-specific ligands than total dissolved Zn found in the NE Atlantic (Ellwood and Van den Berg, 2000). The one part of the surface ocean where this is known not to be the case is the Southern Ocean, (Baars and Croot, 2011), and this is where heavy surface isotopes are not seen.

As shown in the data compilation in Wang et al. (this volume), most profiles with generally negative δ^{66}Zn in the upper ocean actually feature a heavy value right at the surface. In at least some cases, this upward move to heavy Zn isotopes is defined by more than a single sample. We suggest, therefore, that the data are often consistent with uptake of slightly light isotopes at the surface and that the light isotopes that apparently dominate the upper ocean in *e.g.* the North Atlantic (Conway and John, 2014) are at least partially the result of very shallow sub-surface (peaking at about 100 m but extending down to 500 m) regeneration of biomass-associated light Zn isotopes (*e.g.*, Bermin et al., 2006). It is also clear, however, that mass balance considerations mean that such a process cannot explain the overall light upper layer outside the Southern Ocean - *i.e.* the upper 500m. This Southern Ocean biogeochemical divide is emerging as a key feature of the ocean biogeochemistry of Zn, consistent with the behavior of other nutrients in the ocean (*e.g.*, Marinov et al., 2006; Sarmiento et al., 2004; Vance et al., 2017). The Zn-rich deep cycle is fed by deep waters that only re-connect to the surface in the Southern Ocean, and sits below a rather isolated extra-Southern shallow ocean exhibiting different processes. Recent studies have highlighted a very similar pattern for Cd and its isotopes, with Cd isotopes apparently buffered to a surprisingly constant value in this low-latitude surface pool (*e.g.*, Xie et al., 2017; Sieber et al., this volume). It is speculation at present, but the idea that one of the processes that have been invoked for Cd, supply from the atmosphere (Xie et al., 2017), could also explain light Zn in the low latitude surface merits further investigation.

Acknowledgements

We are grateful to Alysia D. Cox for help with setting up a phytoplankton culturing lab at ETH Zurich and to Timothy I. Eglinton for allowing us access to biology laboratories and incubator facilities. We also wish to thank Corey Archer for valuable support with elemental and isotopic analysis and Amélie Ritscher for her work as a research assistant at ETH Zurich. Financial support was provided by ETH and the Swiss National Science Foundation (SNF) through grant 200021-143262.

References

Archer, C., Vance, D., 2004. Mass discrimination correction in multiple-collector plasma source mass spectrometry: an example using Cu and Zn isotopes. Journal of Analytical Atomic Spectrometry, 19: 656-665.

Baars, O., Croot, P.L., 2011. The speciation of dissolved zinc in the Atlantic sector of the Southern Ocean. Deep Sea Research Part II: Topical Studies in Oceanography, 58: 2720-2732.

Ban, Y., Aida, M., Nomura, M., Fujii, Y., 2002. Zinc isotope separation by ligand exchange chromatography using cation exchange resin. Journal of Ion Exchange, 13: 46-52.

Bermin, J., Vance, D., Archer, C., Statham, P.J., 2006. The determination of the isotopic composition of Cu and Zn in seawater. Chemical Geology, 226: 280-297.

Brand, L.E., 1991. Minimum iron requirements of marine phytoplankton and the implications for the biogeochemical control of new production. Limnology and Oceanography, 36: 1756-1771.

Bruland, K.W., 1980. Oceanographic distributions of cadmium, zinc, nickel, and copper in the North Pacific Earth and Planetary Science Letters, 47: 176-198.

Bruland, K.W. (1989) Complexation of zinc by natural organic ligands in the central North Pacific. Limnology and Oceanography 34: 269-285.

Bruland, K.W., Middag, R., Lohan, M.C., 2014. Controls of trace metals in seawater. In: Heinrich, D.H., Karl, K.T. (Eds.), Treatise on Geochemistry. Elsevier, Oxford, pp. 19-51.

Buitenhuis, E.T. et al., 2013. MAREDAT: towards a world atlas of MARine Ecosystem DATa. Earth System Science Data, 5: 227-239.

Cloquet, C., Carignan, J., Lehmann, M., Vanhaecke, F., 2008. Variation in the isotopic composition of zinc in the natural environment and the use of zinc isotopes in biogeosciences: a review. Analytical and Bioanalytical Chemistry, 390: 451-463.

Conway, T.M., John, S.G., 2014. The biogeochemical cycling of zinc and zinc isotopes in the North Atlantic Ocean. Global Biogeochemical Cycles, 28: 1111-1128.

Conway, T.M., John, S.G., 2015. The cycling of iron, zinc and cadmium in the North East Pacific Ocean – insights from stable isotopes. Geochimica et Cosmochimica Acta, 164: 262-283.

Cox, A.D., Saito, M.A., 2013. Proteomic responses of oceanic *Synechococcus* WH8102 to phosphate and zinc scarcity and cadmium additions. Frontiers in Microbiology, 4: 387, pp. 1-17.

Ding, X., Nomura, M., Fujii, Y., 2010a. Zinc isotope effects by chromatographic chelating exchange resin. Progress in Nuclear Energy, 52: 164-167.

Ding, X., Nomura, M., Suzuki, T., Fujii, Y., 2010b. Chromatographic zinc isotope separation by chelating exchange resin. Chromatographia, 71: 195-199.

Domsic, J.F. et al., 2008. Entrapment of Carbon Dioxide in the Active Site of Carbonic Anhydrase II. Journal of Biological Chemistry, 283: 30766-30771.

Ellwood, M.J., Van den Berg, C.M.G., 2000. Zinc speciation in the Northeastern Atlantic Ocean. Marine Chemistry, 68: 295-306.

Falkowski, P.G., Knoll, A.H., 2007. Evolution of primary producers in the sea. Elsevier Academic Press.

Follows, M.J., Dutkiewicz, S., Grant, S., Chisholm, S.W., 2007. Emergent Biogeography of Microbial Communities in a Model Ocean. Science, 315: 1843-1846.

Follows, M.J., Dutkiewicz, S., 2010. Modeling Diverse Communities of Marine Microbes. Annual Review of Marine Science, 3: 427-451.

Gélabert, A. et al., 2006. Interaction between zinc and freshwater and marine diatom species: surface complexation and Zn isotope fractionation. Geochimica et Cosmochimica Acta, 70: 839-857.

Hopkinson, B.M., Barbeau, K.A., 2008. Interactive influences of iron and light limitation on phytoplankton at subsurface chlorophyll maxima in the eastern North Pacific. Limnology and Oceanography, 53: 1303-1318.

John, S.G., Geis, R.W., Saito, M.A., Boyle, E.A., 2007. Zinc isotope fractionation during high-affinity and low-affinity zinc transport by the marine diatom *Thalassiosira oceanica*. Limnology and Oceanography, 52: 2710-2714.

John, S.G., Conway, T.M., 2014. A role for scavenging in the marine biogeochemical cycling of zinc and zinc isotopes. Earth and Planetary Science Letters, 394: 159-167.

John, S.G., Helgoe, J., Townsend, E., 2018. Biogeochemical cycling of Zn and Cd and their stable isotopes in the Eastern Tropical South Pacific. Marine Chemistry 201: 256-262.

Knoll, A.H., Canfield, D.E., Konhauser, K.O. (Eds.), 2012. Fundamentals of Geobiology. John Wiley & Sons, Ltd., pp. 443.

Köbberich, M., Vance, D., 2017. Kinetic control on Zn isotope signatures recorded in marine diatoms. Geochimica et Cosmochimica Acta, 210: 97-113.

Köbberich, M., Vance, D., 2018. Zinc association with surface-bound iron-hydroxides on cultured marine diatoms: A zinc stable isotope perspective. Marine Chemistry.

Leblanc, K. et al., 2012. A global diatom database – abundance, biovolume and biomass in the world ocean. Earth System Science Data, 4: 149-165.

Little, S.H., Vance, D., McManus, J., Severmann, S., 2016. Key role of continental margin sediments in the oceanic mass balance of Zn and Zn isotopes. Geology, 44: 207-210.

Maréchal, C.N., Télouk, P., Albarède, F., 1999. Precise analysis of copper and zinc isotopic compositions by plasma-source mass spectrometry. Chemical Geology, 156: 251-273.

Marinov, I., Gnanadesikan, A., Toggweiler, J.R., Sarmiento, J.L., 2006. The Southern Ocean biogeochemical divide. Nature, 441: 964-967.

Markovic, T. et al., 2017. Experimental determination of zinc isotope fractionation in complexes with the phytosiderophore 2'-deoxymugeneic acid (DMA) and its structural analogues, and implications for plant uptake mechanisms. Environmental Science & Technology, 51: 98–107.

Menemenlis, D. et al., 2005. NASA supercomputer improves prospects for ocean climate research. Eos, Transactions American Geophysical Union, 86: 89-96.

Moore, C.M. et al., 2013. Processes and patterns of oceanic nutrient limitation. Nature Geoscience, 6: 701-710.

Morel, F.M.M., 2008. The co-evolution of phytoplankton and trace element cycles in the oceans. Geobiology, 6: 318-324.

Morel, F.M.M., Milligan, A.J., Saito, M.A., 2014. Marine bioinorganic chemistry: the role of trace metals in the oceanic cycles of major nutrients. In: Heinrich, D.H., Karl, K.T. (Eds.), Treatise on Geochemistry. Elsevier, Oxford, pp. 123-150.

O'Brien, C.J. et al., 2013. Global marine plankton functional type biomass distributions: coccolithophores. Earth System Science Data, 5: 259-276.

Österberg, R., 1974. Origins of metal ions in biology. Nature, 249: 382-383.

Ponzevera, E. et al., 2006. Mass discrimination during MC-ICPMS isotopic ratio measurements: investigation by means of synthetic isotopic mixtures (IRMM-007 series) and application to the calibration of natural-like zinc materials (Including IRMM-3702 and IRMM-651). Journal of the American Society for Mass Spectrometry, 17: 1413-1428.

Roberts, S.B., Lane, T.W., Morel, F.M.M., 1997. Carbonic anhydrase in the marine diatom *Thalassiosira weissflogii* (Bacillariophyceae). Journal of Phycology, 33: 845-850.

582 Saito, M.A., Sigman, D.M., Morel, F.M.M., 2003. The bioinorganic chemistry of the ancient
583 ocean: the co-evolution of cyanobacterial metal requirements and biogeochemical
584 cycles at the Archean–Proterozoic boundary? Inorganica Chimica Acta, 356: 308-318.
585
586 Samanta, M., Ellwood, M.J., Sinoir M., Hassler C.S., 2017. Dissolved zinc isotope cycling in
587 the Tasman Sea, SW Pacific Ocean. Marine Chemistry: 192: 1-12.
588
589 Samanta, M., Ellwood, M.J., Strzepek, R.F., 2017. Zinc isotope fractionation by *Emiliania*
590 *huxleyi* cultured across a range of free zinc ion concentrations. Limnology and
591 Oceanography: 63: 660-671.
592
593 Sarmiento, J.L., Gruber, N., Brzezinski, M.A., Dunne, J.P., 2004. High-latitude controls of
594 thermocline nutrients and low latitude biological productivity. Nature, 427: 56-60.
595
596 Sedwick, P.N., Church, T.M., Bowie, A.R., Marsay, C.M., Ussher, S.J., Achilles, K.M.,
597 Lethaby, P.J., Johnson, R.J., Sarin, M.M., McGillicuddy, D.J. (2005), Iron in the
598 Sargasso Sea (Bermuda Atlantic Time- series Study region) during summer: Eolian
599 imprint, spatiotemporal variability, and ecological implications, Global
600 Biogeochemical Cycles, 19, GB4006.
601
602 Shaked, Y., Xu, Y., Leblanc, K., Morel, F.M.M., 2006. Zinc availability and alkaline
603 phosphatase activity in Emiliania huxleyi: Implications for Zn-P co-limitation in the
604 ocean. Limnology and Oceanography, 51: 299-309.
605
606 Sieber, M., Conway, T.M., de Souza, G.F., Obata, H., Takano, S., Sohrin, Y., Vance, D., in
607 press. Physical and biogeochemical controls on the distribution of dissolved cadmium
608 and its isotopes in the Southwest Pacific Ocean. Chemical Geology, this volume.
609
610 Siebert, C., Nägler, T.F., Kramers, J.D., 2001. Determination of molybdenum isotope
611 fractionation by double-spike multicollector inductively coupled plasma mass
612 spectrometry. Geochemistry, Geophysics, Geosystems, 2: 1032.
613
614 Six, C. et al., 2007. Diversity and evolution of phycobilisomes in marine *Synechococcus spp.*: a
615 comparative genomics study. Genome Biology, 8: R259 pp. 1-22.
616
617 Smayda, T.J., 1978. From phytoplankters to biomass. In: Sournia, A. (Ed.), Phytoplankton
618 manual. Museum National d'Histoire Naturelle, Paris, pp. 273-279.
619
620 Sun, J., Liu, D., 2003. Geometric models for calculating cell biovolume and surface area for
621 phytoplankton. Journal of Plankton Research, 25: 1331-1346.
622
623 Sunda, W.G., Huntsman, S.A., 1992. Feedback interactions between zinc and phytoplankton in
624 seawater. Limnology and Oceanography, 37: 25-40.
625
626 Sunda, W.G., Huntsman, S.A., 1995. Iron uptake and growth limitation in oceanic and coastal
627 phytoplankton. Marine Chemistry, 50: 189-206.
628

Sunda, W.G., Huntsman, S.A., 1997. Interrelated influence of iron, light and cell size on marine phytoplankton growth. Nature, 390: 389-392.

Sunda, W.G., Price, N.M., Morel, F.M.M., 2005. Trace metal ion buffers and their use in culture studies. In: Andersen, R.A. (Ed.), Algal Culturing Techniques. Academic Press, Burlington.

Sunda, W., Huntsman, S., 2015. High iron requirement for growth, photosynthesis, and low-light acclimation in the coastal cyanobacterium *Synechococcus bacillaris*. Frontiers in Microbiology, 6: 561.

Tang, D., Morel, F.M.M., 2006. Distinguishing between cellular and Fe-oxide-associated trace elements in phytoplankton. Marine Chemistry, 98: 18-30.

Twining, B.S. et al., 2003. Quantifying trace elements in individual aquatic protist cells with a synchrotron X-ray fluorescence microprobe. Analytical Chemistry, 75: 3806-3816.

Twining, B.S., Baines, S.B., 2013. The trace metal composition of marine phytoplankton. Annual Review of Marine Science, 5: 191-215.

Vance, D. et al., 2016a. The oceanic budgets of nickel and zinc isotopes: the importance of sulfidic environments as illustrated by the Black Sea. Philosophical Transactions of the Royal Society A: Mathematical, Physical and Engineering Sciences, 374: 1-26.

Vance, D. et al., 2016b. The behaviour of Cu and Zn isotopes during soil development: controls on the dissolved load of rivers. Chemical Geology, 445: 36-53.

Vance, D. et al., 2017. Silicon and zinc biogeochemical cycles coupled through the Southern Ocean. Nature Geoscience, 10: 202-206.

Wang, R.M., Archer, C., Bowie, A.R., Vance, D., in press. Zinc and nickel isotopes in seawater from the Indian Sector of the Southern Ocean: the impact of natural iron fertilization versus Southern Ocean hydrography and biogeochemistry. Chemical Geology, this volume.

Wolfe-Simon, F., Grzebyk, D., Schofield, O., Falkowski, P.G., 2005. The role and evolution of superoxide dismutases in algae. Journal of Phycology, 41: 453-465.

Xie, R.C., Galer, S.J.G., Abouchami, W., Rijkenberg, M.J.A., de Baar, H.J.W., De Jong, J., Andreae, M.O., 2017. Non-Rayleigh control of upper-ocean Cd isotope fractionation in the western South Atlantic, Earth and Planetary Science Letters, 471: 94-103.

Zhao, Y., 2011. The carbon cycle and bioactive trace metals in the oceans: constraints from zinc isotopes. Dissertation, University of Bristol.

674 Zhao, Y., Vance, D., Abouchami, W., de Baar, H.J.W., 2014. Biogeochemical cycling of zinc
675 and its isotopes in the Southern Ocean. Geochimica et Cosmochimica Acta, 125: 653-
676 672.

677

Figure captions

full page: **Table 1.** Measured Fe and Zn uptake rates, cellular quotas, use efficiencies, and Zn isotope results ($\Delta^{66}Zn_{\text{biomass - medium}} = \delta^{66}Zn_{\text{biomass}} - \delta^{66}Zn_{\text{medium}}$).

two-column fitting image: **Fig. 1.** Comparison of surface area to biovolume (A/V) ratios for all phytoplankton cultured here to the ranges observed in natural communities as derived from MARine Ecosystem DATa (MAREDAT; Buitenhuis et al., 2013).

single-column fitting image: **Fig. 2.** Specific growth and metal uptake rates as a function of A/V ratios for all cultured diatoms and cyanobacteria.

single-column fitting image: **Fig. 3.** Cellular Fe and Zn quotas as a function of A/V ratios (A and B) and their interdependency (C) for all cultured diatoms and cyanobacteria.

single-column fitting image: **Fig. 4.** $\Delta^{66}Zn$ fractionation of cyanobacteria, which are variably well adapted to the applied nutrient and light conditions as a result of their different light harvesting strategies.

two-column fitting image: **Fig. 5.** Comparison of the Zn isotope fractionation upon uptake for all phytoplankton studied here, along with data from the literature. The red band indicates the range of $\Delta^{66}Zn$ values that could be explained simply by the presence of EDTA as a strong organic chelator in the culture medium, and published data for Zn isotope separation between Zn-EDTA and Zn^{2+} (Ban et al., 2002; Ding et al., 2010a; Ding et al., 2010b; Markovic et al., 2017).

Supplementary Information

Associated with:

Zn isotope fractionation during uptake into marine phytoplankton: implications for oceanic zinc isotopes

Michael Köbberich[1*] and Derek Vance[1]

*To whom correspondence should be addressed

Submitted to: ***Chemical Geology***

Special issue: ***GEOTRACES - Goldschmidt Session 10i***

S.1 A novel artificial *Prochlorococcus* medium

In common with previous work (Anderson et al., 1978; Berges et al., 2001; Harrison et al., 1990; Morel et al., 1979; Price et al., 1989; Sunda et al., 2005), the strong chelating agent, EDTA, was used to maintain constant and low bioavailable Zn levels over the course of all culture experiments conducted here. The use of constant EDTA concentrations (at around 100 μmol l^{-1}) simplifies not only inter-species comparison but also direct comparison with published work. From a Zn stable isotope perspective, EDTA has previously been suggested to drive the bioavailable metal pool towards lighter isotope compositions, as heavy Zn isotopes are preferentially associated with the chelating agent (John et al., 2007; Köbberich and Vance, 2017). Since the addition of any organic compound bears the risk of affecting the isotopic composition of bioavailable Zn, we sought to avoid natural seawater bases and to keep EDTA high (at around 100 μmol l-1; Sunda et al., 2005) and as close to constant as possible, to avoid further complications potentially caused by the distribution of Zn isotopes among aqueous species. All media previously used for culturing Prochlorococcus (Chisholm, 1992; Laloui et al., 2002; Moore et al., 2007; Moore et al., 1998; Rippka et al., 2000) have furthermore involved EDTA concentrations a factor of 8 lower than this. In brief, the artificial *Prochlorococcus* medium used here differs from that used for the other organisms cultured here in the following key features: its nitrogen (N) source, total molybdenum and selenium concentrations, its trace metal buffer capacity, and consequently the bioavailable concentrations of all divalent metals.

As none of the currently known isolates has been reported to grow on nitrate, N was supplied as ammonia, by means of ammonium chloride salt, adjusted to yield a final concentration of 538 μmol l^{-1}. Analogous to the widely used enriched natural seawater PRO99 (Moore et al., 2007; Moore et al., 2002), total molybdenum (Mo) and selenium (Se) concentrations were set to elevated – for culture media – levels of 3 and 10 nmol l^{-1}, respectively. In contrast to PRO99, but identical to the broad-spectrum medium used for the other organisms (Section 2.1), Mo stock solutions were prepared with Na_2MoO_4, while those of Se were made from a hydrated

$Na_2SeO_3 \cdot 5\ H_2O$ salt. Given increased EDTA concentrations of 100 µmol l^{-1}, while total concentrations of all divalent cations in PRO99 remain unmodified, the non-complexed bioavailable metal fraction would be lowered. In a series of preliminary experiments, we found that this increased degree of trace metal buffering by EDTA caused insufficient *Prochlorococcus* growth, pointing to the need to adapt the overall trace metal balance. The total concentrations of the transition metals iron (Fe), cobalt (Co), nickel (Ni), and copper (Cu) were therefore adjusted to yield Me′ levels of about 250, 100, 50, and 0.5 pmol l^{-1}, respectively. The abundance of Zn′ at the given EDTA content is 138 pmol l^{-1} and that of Zn^{2+} 91 pmol l^{-1}.

Growth rates of the cultured *Prochlorococcus* were found to be low compared to values for this clone in Moore and Chisholm (1999), who also report the optimum light level for this clone to be around 100 µmol photons m^{-2} s^{-1}. Here we observed maximum growth at much lower light levels of < 30 µmol photons m^{-2} s^{-1} with insignificant growth at 50 µmol photons m^{-2} s^{-1}. The observed difference is likely to be caused by the use of a fundamentally different synthetic seawater solution. For example, Moore and Chisholm (1999) enriched natural seawater with nutrients.

S.2 Diffusion limitation: Theory & Calculation

Resource supply to a phytoplankton cell becomes diffusion limited as soon as the cellular uptake rate of that resource exceeds the maximum rate of supply via diffusion through the medium. Early work noted that large diatoms (small surface area / biovolume ratios, *c.f.* Fig. S.1A) are often more prone to becoming diffusion limited, in cultures with identical bioavailable Zn concentrations, than much smaller cells (Sunda and Huntsman, 1992). Light isotopes of Zn have been shown experimentally to diffuse slightly faster than heavier isotopes (Rodushkin et al., 2004), a process that could potentially lead to the enrichment of the light isotopes of Zn in phytoplankton cells (John et al., 2007; Samanta et al., 2017). Given that the aim of this study is to compare different sized phytoplankton with respect to Zn isotope effects associated with the specific process of cellular uptake, rather than as a result of diffusion-induced gradients in the medium, it becomes important to prevent diffusion limitation in all

cultures prepared for comparison. It was, thus necessary to identify a set of culturing conditions that allows comparison of the widest possible range of differently sized phytoplankton whilst ensuring that the Zn isotope composition of the diffusion limitation does not occur across the size range.

Whether an individual cell becomes diffusion limited depends on a range of parameters: cell size but also the ambient Zn′ level, the specific growth rate (μ), and the amount of Zn taken up per cell (as recorded *e.g.* by cellular Zn/P ratios). The cellular dimension and geometries of MAREDAT diatoms (Leblanc et al., 2012) and coccolithophores (O'Brien et al., 2013) were used to explore the impact of size and key culturing parameters on the percentage of cells that are diffusion limited. Biomass Zn/P ratios were assumed to be around 2 mmol mol^{-1}, the mean intra-cellular value for various natural communities (Twining and Baines, 2013; Twining et al., 2003) and found in previous culture experiments (Sunda and Huntsman, 1992). These Zn/P ratios were converted to absolute cellular Zn quotas using previously-suggested empirical relationships for calculating the carbon biomass from cell volumes (Leblanc et al., 2012; Smayda, 1978; Sun and Liu, 2003) and a Redfield C/P ratio of 106/1.

The maximum diffusion rate (ρ) was assessed using $\rho = 4\pi rD$ [Me′], where [Me′] represents the inorganic metal concentration in the medium outside the cell. The radius (r) was derived from the biovolume by assuming all cells to be spherical (Sunda and Huntsman, 1992). Values of $6 \cdot 10^{-6}$ cm^2 s^{-1} (Sunda and Huntsman, 1992) and $9 \cdot 10^{-6}$ cm^2 s^{-1} (Hudson and Morel, 1990) were used for the diffusion rate constant (D) of Zn and Fe, respectively.

As a result of this (rather strict) assessment, Zn′ was set to a value of about 0.1 nmol l^{-1}. Two thirds of all the 1362 MAREDAT diatoms and 181 coccolithophores are not diffusion limited at this Zn concentration, up to growth rates of 0.8 d^{-1}, and for cellular Zn/P ratios <2 mmol mol^{-1} (Fig. S.1B). This Zn' concentration is above the threshold where diffusion limited uptake of Zn starts to matter, for a variety of differently sized phytoplankton. Conversely, the proportion of phytoplankton not limited by diffusion is higher the less Zn is taken up into the cell (Fig. S.1C), or the slower the growth (Fig. S.1D), assuming the other two parameters to remain constant. In

this context, it is important to keep in mind that the definition applied here of where diffusion limitation begins in rather strict. Underlying our definition is the assumption that the surface is 100% covered in Zn transporters, which is of course not possible as there must be transporters of other nutrients too, as well as structural proteins, phospholipids, and other cell wall components. Sunda and Huntsman (1992) thus suggest that diffusion limitation of *E. huxleyi* and *T. pseudonana* might begin as early as at ~ 30% of the maximum diffusive flux (Hudson and Morel, 1993). In the light of such considerations it important not to get to close to the calculated concentration threshold in culture experiments that are not designed to be diffusion limited.

This can also be examined from the perspective of cellular A/V ratios. If similar cellular Zn quotas taken up into smaller *versus* larger cells, small cells (large A/V ratio) will begin to suffer from diffusion limitation at lower Zn′ (Fig. S.1E) compared to larger cells (small A/V ratio). It is important to note that this theoretically predicted effect is typically compensated by the fact that small cells grow much more slowly than larger ones, and that often they also do not take up as much Zn. For *T. weissflogii*, the largest diatom studied here, Zn′ concentrations as low as 0.01 nmol l^{-1} would come with severe diffusion limitation (red square in Fig. S.1A). On the other hand, at the chosen Zn′ level of 0.1 nmol l^{-1}, cellular Zn/P ratios can be as high as 4 mmol mol^{-1} (Fig. S.1F), and growth rates as high as 1.6 d^{-1} (Fig. S.1G), without diffusion limitation of Zn uptake in *T. weissflogii*. However, it worth noting that a unimodal relationship between phytoplankton growth rate and cell size has previously been described by Chen and Liu (2010), when temperature and nutrient availability are accounted for.

S.3 UV-VIS-NIR absorbance spectrophotometry and *in vivo* fluorescence

An important aim of this contribution is to explore species dependent isotope effects associated with Zn uptake into the cell, covering the diversity of cyanobacteria to the greatest possible extent. In order to achieve this aim, robust criteria are needed to distinguish the different strains. Large eukaryotic phytoplankton tends to offer criteria that can be used for discrimination, which also help to distinguish ecologically and evolutionary distinct species.

For prokaryotes, by contrast visual features, detectable *e.g.* by light microscopy, are often ambiguous. Instead, molecular methods such as the sequencing of nucleic acids are commonly used to capture diversity among prokaryotes. To some degree, the budgets of different photosynthetic pigments in cultured cells can be used. The color of dense monocultures can provide a first indication of the cellular budget of photosynthetic pigments in cyanobacteria, and thus the identity of the organism. The absorbance of ultraviolet (UV), visible (VIS), and near-infrared (NIR) light, together with *in vivo* fluorescence in response to monochromatic light, can provide further information on the photo-physiological capabilities and the molecular structure of the light harvesting apparatus in living cyanobacterial cells.

A combination of UV-VIS-NIR and *in vivo* fluorescence (Supplementary Figure S.2) was thus used to verify that all four of the cyanobacteria here are distinct in the molecular structure and composition of their light harvesting complexes, namely their phycobilisomes. The molecular structure of the light harvesting apparatus is not only resulting the complex evolutionary history of prokaryotes, it also significantly contributes to the color of dense monocultures. *Prochlorococcus marinus* and three *Synechococcus* strains (see Section 2.1) were chosen to cover a range of different colors, reflecting structural differences in their photosynthetic apparatus. Two of the chosen *Synechococcus* strains (CCMP 1334 and 2370; Scanlan et al., 2009; Six et al., 2007; Six et al., 2005; Six et al., 2004; Toledo et al., 1999) and *P. marinus* (CCMP 2389; Biller et al., 2015; Moore et al., 1995; Scanlan et al., 2009; Ting et al., 2002) were previously well characterized with respect to their light harvesting architecture. Unlike other green strains such as CCMP 1333 (*a.k.a.* WH 5701, see *e.g.*, Six et al., 2007), the green representative of the genus *Synechococcus* (CCMP 1183) used here has not previously been shown to have a phycocyanin dominated phyobiliprotein composition.

All spectrofluorometric *in vivo* analyses were done during exponential growth phase using an Infinite® 200 Pro plate reader (Tecan, Switzerland). Absorbance spectra were recorded for the wavelength range 350 to 750 nm, in step sizes of 1 nm (Supplementary Figure S.2). The blank corrected absorbance of every species was individually normalized to the measurement with the

least transmittance. The excitation wavelength chosen to obtain fluorescence spectra was set to the observed absorbance maxima and hence to values of 390, 415, 440, 495, 550, and 630 nm, for all four cyanobacteria strains. Fluorescence readings were typically recorded from 800 nm down to 30 nm above the excitation wavelength, in a step size of 2 nm, with emission intensities integrated over 20 μs. Inter-species differences in absolute intensities were preserved by normalizing all fluorescence data to the maximum emission recorded among all four cyanobacteria strains.

S.4 Distinguishing cyanobacteria *via* their photosynthetic apparatus

All studied phytoplankton is harvesting light with antenna complexes, called phycobilisomes, which are differing in their molecular structure between different organisms. Classification of all here investigated strains to groups of distinct light harvesting strategies was confirmed using previously established techniques. The framework for doing this was established by Six et al. (2007) for evolutionary distinct *Synechococcus* strains, which were then compared to *Prochlorococcus marinus* following Moore et al. (1995), Ting et al. (2002) and Biller et al. (2015).

Synechococcus cells owe their vivid colors (Fig. S.3A) to the macromolecular structure of their phycobilisomes (Glazer, 1989; Glazer et al., 1985), with rods made of phycobiliproteins surrounding a central allophycocyanin core (Scanlan et al., 2009; Six et al., 2007). Only in some *Synechococcus* strains does phycocyanin (PC) constitute the whole rod (Type 1 according to Six et al., 2007): in most cases PC only makes up the basal end of the rod while most of it is phycoerythrin (Fig. S.3B; Type 2 and 3 according to Six et al., 2007). All type 3 strains, however, contain the red and orange colored chromophores phycoerythrobilin (PEB, A_{max} = 550 nm) and phycourobilin (PUB, A_{max} = 495 nm) in variable proportions (Fig. S.3C), according to their preferred light niche. The *Synechococcus* strain CCMP 1183 has not previously been categorized into any of these types, while CCMP 1334 and 2370 are known to be of type 3a and 3c, respectively (Six et al., 2007). Six et al. (2007) recommend distinguishing the latter two types using fluorescence excitation maxima ($F_{495\ nm}$ / $F_{550\ nm}$) emitting at around

580 nm, since the carotenoids zeaxanthin and β-carotene interfere with the characteristic absorbance ratio ($A_{495\ nm}$ / $A_{550\ nm}$). For CCMP 1334 and 2370, PUB / PEB ratios are 0.457 and 1.829, as obtained with white light, and are in very good in agreement with previously reported values of 0.440 and 1.856 (Six et al., 2007). The lack of fluorescence emitted at 580 nm ruled out types 2 or 3 due to the absence of phycoerythrin in CCMP 1183, while pronounced emissions at ~660 nm, excited at ~630 nm, indicate the dominance of PC instead (Type 1).

Prochlorococcus marinus (CCMP 2389) is well known be one of the few cyanobacteria strains (together with *Prochloron and Prochlorothrix*) that lack phycobilisomes (Fig. S.3B; Biller et al., 2015), but possesses a divinyl chlorophyll a and b binding protein (Biller et al., 2015; Chisholm et al., 1992). Significant proportions of this pigment typically express a lime-green color in dense pure *Prochlorococcus* cultures (Fig. S.3D; Lindell, 2014). This distinctive pigmentation supports more efficient absorption of green light due to a blue-light absorbance maximum which, in comparison to other phycoerythrin free species (*e.g.*, CCMP 1183), is shifted towards higher wavelength (Fig. S.3C).

S.5 Speculations on the anomalous metal quotas and Δ^{66}Zn of CCMP 2370

Cox and Saito (2013), found that relative metallothionein (MT) abundances rose when Zn was added to CCMP 2370 cultures, and that this was accentuated at low PO_4^{3-}. This suggests the possibility of a link to PO_4^{3-} acquisition, since alkaline phosphatases (PhoA) require Zn. High cellular MT contents could thus also explain high biomass Zn/P ratios, as observed for CCMP 2370. Although an explanation for the exact use of MT is still elusive (Palmiter, 1998), two functionalities seem likely. Firstly, MT could build up a cellular Zn reservoir, serve as a chaperon to transport Zn to Zn-containing proteins, and ultimately detoxify the cell if intracellular divalent metal contents get too high. Secondly, it has also been suggested as a potentially very powerful antioxidant, preventing accumulation of oxygen (O) radicals (Cox and Saito, 2013; Palmiter, 1998; Robinson et al., 2001). Zn in MT is four-fold coordinated via thiol groups, or is arranged in more complex ZnS clusters of variable structure and stoichiometry (Maret et al., 1997; Maret and Vallee, 1998). If published *ab-initio* calculations

of the equilibrium isotope fractionation between Zn^{2+} and the amino acid cysteine (Fujii et al., 2014) are representative for such clusters, one could speculate that they would preferentially bind heavy Zn isotopes. If Zn efflux from the cell derives exclusively from the non-MT-bound intracellular Zn pool, this could cause enrichment of heavy Zn-isotopes in the phytoplankton cell, while light Zn is continuously re-exported to the ambient medium. Dupont et al. (2008) show that clone CCMP 2370 has a strong requirement for Ni in superoxide dismutase (SOD) but does not have the genes for Zn or Cu SOD. The necessity to detoxify an excess of intracellular Zn might thus also differentiate CCMP 2370 from the other studied strains.

Phycourobilin PUB has a light absorption maximum at a wavelength of around 495 nm (blue-green). In coastal settings, where scattering by particles significantly reduces light penetration depth, this is the part of the light spectrum that reaches deepest into the water column (Wozniak and Dera, 2007). One could speculate that CCMP 2370 is possibly better adapted to deeper open ocean or coastal ecological niches compared to the other *Synechococcus* strains (not *Prochlorococcus*). Such environments, both deep open marine and coastal, are often Zn-rich in comparison to the shallowest open ocean. A metabolism that is evolutionarily adapted to such an environment would not necessarily need to economize its Zn use. It is perhaps noteworthy, then, that *P. marinus* is perhaps one of the best documented examples of a cyanobacterium that persists deeper in the water column. The high-light adapted strain used for experimentation here, however, originates from a water depth of only 5 m in the Mediterranean and might not be representative of depth-adapted *Prochlorococcus* cells.

An alternative irradiance-based scenario to explain unusually high Zn quotas associated with CCMP 2370 could be that the irradiance levels used in culture are the farthest away from the natural habitat of this strain. Finkel et al. (2006) consistently observe higher cellular Zn and Fe quotas among various light limited phytoplankton, but this seems unlikely to explain the data for CCMP 2370 as its type 3c photosynthetic apparatus should still allow it to capture blue-green light when other phototrophs might become growth limited. The culture experiment here was done with white light. Given that CCMP 2370 might be adapted to a blue-green niche, it

seems imaginable that inappropriate light-spectra might cause similar effects. Currently, it can only be speculated about possible mechanisms, but the need to detoxify the cell of unwanted photosynthetic by-products, such as oxygen radicals, by means of Zn-containing proteins (Cox and Saito, 2013; Palmiter, 1998) could be one way to explain the higher cellular Zn budget.

S.6 Fe and Zn use efficiencies of pro- *versus* eukaryotes

Sunda and Huntsman (2015) further developed a scheme, first established by Raven (1990), that allows computing how much atmospheric CO_2 is fixed into marine biomass per Fe atom. The coastal diatom *Thalassiosira pseudonana* was previously found to build up more biomass per Fe atom than the cyanobacterium *Synechococcus bacillaris* (Sunda and Huntsman, 2015). In other words, eukaryotic diatoms tend to use Fe more efficiently than prokaryotic cyanobacteria. Analogous to this approach, we calculate the iron use efficiency (IUE) by dividing the specific growth rate of an organism by its cellular Fe/P ratio. The interest in comparing IUEs among different phytoplankton originates with the hypothesis that modern prokaryotes require higher cellular Fe contents, as a vestige from the time when they first evolved in a primordial ocean rich in Fe, later than eukaryotes.

In contrast to Fe, the Precambrian ocean is assumed to be lower in its Zn inventory than the modern (Anbar, 2008; Zerkle et al., 2005), posing the question of whether the cellular Zn content of phytoplankton would then also need to be the reverse of Fe (Saito et al., 2003). Our cellular Fe and Zn quotas seem to support both hypotheses (Fig. 3A and B), with the caveat that one cyanobacterial strain records the highest measured Zn/P ratio in the entire dataset (CCMP 2370, *c.f.* Section 4.1 and 4.2). IUEs provide an important advantage over absolute cellular quotas in that they consider specific growth rates in their calculation routine. If growth is suppressed in culture because laboratory conditions differ from the natural habitat, which is supposedly the case for CCMP 2370, this is partly accounted for by IUEs. It is only 'partly' accounted for, as the cell might still have needed to adapt its metallo-proteome to achieve the observed growth rate. But, without proteomic data, usage efficiencies might be as close as one currently can get to quantifying species-dependent differences independent of environmental

255 factors. Here, we thus take this concept further and extend it to zinc use efficiencies (ZUE),
256 which we use to further explore the dependency of both metal usage efficiencies on the cellular
257 metal quota and those of the other element, respectively.

258 Both IUE and ZUE decrease with increasing cellular Fe and Zn quotas (Fig. S.4A and B). The
259 highest Zn use efficiencies were observed in representatives of the prokaryotic genus
260 *Synechococcus* with Fe/P ratios in the range between ~4 and 5.5 mmol mol^{-1} (Fig. S.4C). The
261 biomass elements C and P, in contrast, are most efficiently built up per Zn atom in eukaryotic
262 marine diatoms with cellular Zn/P ratios of ~1.5 to 2 mmol mol^{-1} (Fig. S.4D). This behavior is
263 in strong contrast to what can be observed for Fe and Zn uptake rates (Fig. S.4E and F), where
264 diatoms consistently transport most metals per surface area and unit time. It is an intriguing –
265 though unexplained – observation that the most efficient metal usage coincides almost exactly
266 with the numbers that previously reported as the global average of intracellular Fe and Zn
267 quotas of phytoplankton (Fig. S.4C and D), as obtained from synchrotron-based X-ray
268 fluorescence imaging techniques (*e.g.*, Twining and Baines, 2013).

269 Based on the coupling of Zn and Fe uptake rates in an Fe-limitation scenario both metals were
270 previously speculated to be physiologically linked to each other in marine diatoms (Köbberich
271 and Vance, 2017). The metal use efficiencies explored here might shed further light on this
272 idea. It might thus not be coincident that ZUEs are highest around the global average of
273 intracellular Fe/P ratios (Fig. S.4C), while IUEs peak around the global average of intracellular
274 Zn/P (Fig. S.4D). This raises the question as to whether global average cellular quotas are the
275 natural consequence of a potentially rather narrow physiological window that allows the most
276 efficient build-up of bio-elements. Consistent with the hypothesis that modern prokaryotes
277 require higher cellular Fe contents than later evolved eukaryotes, all diatoms studied here were
278 consistently found to use Fe more efficiently than most cyanobacteria, except CCMP 2370 (Fig.
279 S.4D).

280 It is, however, important to note that metal use efficiencies, as calculated by dividing the
281 growth rate by a cellular quota, are minimum estimates. Proper characterization of these values

requires growth under nutrient limitation. The set of experiments presented here was performed at a single pair of Fe and Zn concentrations, so it cannot conclusively be determined whether a strain uses Zn inefficiently, or if cells use Zn at high efficiency but with a large amount of Zn storage. One might infer from Table 1 that *Prochlorococcus* has a lower Zn use efficiency, but there is no evidence that *Prochlorococcus* requires Zn to grow, meaning it could have an infinitely high Zn use efficiency (Saito & Moffett, 2001).

References

Anderson, M.A., Morel, F.M.M., Guillard, R.R.L., 1978. Growth limitation of a coastal diatom by low zinc ion activity. Nature, 276: 70-71.

Berges, J.A., Franklin, D.J., Harrison, P.J., 2001. Evolution of an artificial seawater medium: improvements in enriched seawater, artificial water over the last two decades. Journal of Phycology, 37: 1138-1145.

Biller, S.J., Berube, P.M., Lindell, D., Chisholm, S.W., 2015. Prochlorococcus: the structure and function of collective diversity. Nature Reviews Microbiology, 13: 13-27.

Chen, B., Liu, H., 2010. Relationships between phytoplankton growth and cell size in surface oceans: Interactive effects of temperature, nutrients, and grazing. Limnology and Oceanography, 55: 965-972.

Chisholm, S., 1992. Phytoplankton Size. In: Falkowski, P., Woodhead, A., Vivirito, K. (Eds.), Primary Productivity and Biogeochemical Cycles in the Sea. Environmental Science Research. Springer, pp. 213-237.

Cox, A.D., Saito, M.A., 2013. Proteomic responses of oceanic *Synechococcus* WH8102 to phosphate and zinc scarcity and cadmium additions. Frontiers in Microbiology, 4: 387, pp. 1-17.

Dupont, C.L., Barbeau, K., Palenik, B., 2008. Ni uptake and limitation in marine *Synechococcus* strains. Applied and environmental microbiology, 74: 23-31.

Finkel, Z.V. et al., 2006. Irradiance and the elemental stoichiometry of marine phytoplankton. Limnology and Oceanography, 51: 2690-2701.

Fujii, T., Moynier, F., Blichert-Toft, J., Albarède, F., 2014. Density functional theory estimation of isotope fractionation of Fe, Ni, Cu, and Zn among species relevant to geochemical and biological environments. Geochimica et Cosmochimica Acta, 140: 553-576.

Glazer, A.N., 1989. Light guides. Directional energy transfer in a photosynthetic antenna. Journal of Biological Chemistry, 264: 1-4.

Glazer, A.N., Chan, C., Williams, R.C., Yeh, S.W., Clark, J.H., 1985. Kinetics of Energy Flow in the Phycobilisome Core. Science, 230: 1051-1053.

Harrison, P.J., Thompson, P.A., Calderwood, G.S., 1990. Effects of nutrient and light limitation on the biochemical composition of phytoplankton. Journal of Applied Phycology, 2: 45-56.

Hudson, R.J.M., Morel, F.M.M., 1990. lron transport in marine phytoplankton: kinetics of cellular and medium coordination reactions. Limnology and Oceanography, 35: 1002-1020.

Hudson, R.J.M., Morel, F.M.M., 1993. Trace metal transport by marine microorganisms: implications of metal coordination kinetics. Deep Sea Research, 20: 129-150.

John, S.G., Geis, R.W., Saito, M.A., Boyle, E.A., 2007. Zinc isotope fractionation during high-affinity and low-affinity zinc transport by the marine diatom *Thalassiosira oceanica*. Limnology and Oceanography, 52: 2710-2714.

Köbberich, M., Vance, D., 2017. Kinetic control on Zn isotope signatures recorded in marine diatoms. Geochimica et Cosmochimica Acta, 210: 97-113.

Laloui, W. et al., 2002. Genotyping of axenic and non-axenic isolates of the genus Prochlorococcus and the OMF-'Synechococcus' clade by size, sequence analysis or RFLP of the Internal Transcribed Spacer of the ribosomal operon. Microbiology, 148: 453-465.

Leblanc, K. et al., 2012. A global diatom database – abundance, biovolume and biomass in the world ocean. Earth System Science Data, 4: 149-165.

Lindell, D., 2014. The Genus Prochlorococcus, Phylum Cyanobacteria. In: Rosenberg, E., DeLong, E., Lory, S., Stackebrandt, E., Thompson, F. (Eds.), The Prokaryotes. Springer Berlin Heidelberg, pp. 829-845.

Maret, W., Larsen, K.S., Vallee, B.L., 1997. Coordination dynamics of biological zinc "clusters" in metallothioneins and in the DNA-binding domain of the transcription factor Gal4. Proceedings of the National Academy of Sciences, 94: 2233-2237.

Maret, W., Vallee, B.L., 1998. Thiolate ligands in metallothionein confer redox activity on zinc clusters. Proceedings of the National Academy of Sciences, 95: 3478-3482.

Moore, L.R., Goericke, R., Chisholm, S.W., 1995. Comparative physiology of Synechococcus and Prochlorococcus: influence of light and temperature on growth, pigments, fluorescence and absorptive properties. Marine Ecology Progress Series, 116: 259-275.

Moore, L.R., Rocap, G., Chisholm, S.W., 1998. Physiology and molecular phylogeny of coexisting Prochlorococcus ecotypes. Nature, 393: 464-7.

Moore, L.R., Chisholm, S.W., 1999. Photophysiology of the marine cyanobacterium Prochlorococcus: Ecotypic differences among cultured isolates, Limnology and Oceanography, 44, 628–638.

Moore, L.R., Post, A.F., Rocap, G., Chisholm, S.W., 2002. Utilization of different nitrogen sources by the marine cyanobacteria *Prochlorococcus* and *Synechococcus*. Limnology and Oceanography, 47: 989–996.

Moore, L.R. et al., 2007. Culturing the marine cyanobacterium *Prochlorcoccus*. Limnology and Oceanography: Methods, 5: 353-362.

Morel, F.M.M., Rueter, J.G., Anderson, D.M., Guillard, R.R.L., 1979. AQUIL: a chemically defined phytoplankton culture medium for trace metal studies. Journal of Phycology, 15: 135-141.

O'Brien, C.J. et al., 2013. Global marine plankton functional type biomass distributions: coccolithophores. Earth System Science Data, 5: 259-276.

Palmiter, R.D., 1998. The elusive function of metallothioneins. Proceedings of the National Academy of Sciences, 95: 8428-8430.

Price, N.M. et al., 1989. Preparation and chemistry of the artificial algal culture medium Aquil. Biological Oceanography, 6: 443-461.

Raven, J.A., 1990. Predictions of Mn and Fe use efficiencies of phototrophic growth as a function of light availability for growth and of C assimilation pathway. New Phytologist, 116: 1-18.

Rippka, R. et al., 2000. Prochlorococcus marinus Chisholm et al. 1992 subsp. pastoris subsp. nov. strain PCC 9511, the first axenic chlorophyll a2/b2-containing cyanobacterium (Oxyphotobacteria). International Journal of Systematic and Evolutionary Microbiology, 50: 1833-1847.

Robinson, N.J., Whitehall, S.K., Cavet, J.S., 2001. Microbial metallothioneins, Advances in Microbial Physiology. Academic Press, pp. 183-213.

Rodushkin, I., Stenberg, A., Andrén, H., Malinovsky, D., Baxter, D.C., 2004. Isotopic fractionation during diffusion of transition metal ions in solution. Analytical Chemistry, 76: 2148-2151.

Saito, M.A., Moffett, J.W., 2001. Complexation of cobalt by natural organic ligands in the Sargasso Sea as determined by a new high-sensitivity electrochemical cobalt speciation method suitable for open ocean work. Marine chemistry, 75: 49-68.

Saito, M.A., Sigman, D.M., Morel, F.M.M., 2003. The bioinorganic chemistry of the ancient ocean: the co-evolution of cyanobacterial metal requirements and biogeochemical cycles at the Archean–Proterozoic boundary? Inorganica Chimica Acta, 356: 308-318.

Samanta, M., Ellwood, M.J., Strzepek, R.F., 2017. Zinc isotope fractionation by *Emiliania huxleyi* cultured across a range of free zinc ion concentrations. Limnology and Oceanography: 63: 660-671.

Scanlan, D.J. et al., 2009. Ecological Genomics of Marine Picocyanobacteria. Microbiology and Molecular Biology Reviews, 73: 249-299.

Six, C. et al., 2007. Diversity and evolution of phycobilisomes in marine Synechococcusspp.: a comparative genomics study. Genome Biology, 8: R259.

Six, C. et al., 2005. Two Novel Phycoerythrin-Associated Linker Proteins in the Marine Cyanobacterium *Synechococcus* sp. Strain WH8102. Journal of Bacteriology, 187: 1685-1694.

Six, C., Thomas, J.C., Brahamsha, B., Lemoine, Y., Partensky, F., 2004. Photophysiology of the marine cyanobacterium Synechococcus sp. WH8102, a new model organism. Aquatic Microbial Ecology 35: 17-29.

Smayda, T.J., 1978. From phytoplankters to biomass. In: Sournia, A. (Ed.), Phytoplankton manual. Museum National d'Histoire Naturelle, Paris, pp. 273-279.

Sun, J., Liu, D., 2003. Geometric models for calculating cell biovolume and surface area for phytoplankton. Journal of Plankton Research, 25: 1331-1346.

Sunda, W.G., Huntsman, S.A., 1992. Feedback interactions between zinc and phytoplankton in seawater. Limnology and Oceanography, 37: 25-40.

Sunda, W., Huntsman, S., 2015. High iron requirement for growth, photosynthesis, and low-light acclimation in the coastal cyanobacterium *Synechococcus bacillaris*. Frontiers in Microbiology, 6: 561.

Sunda, W.G., Price, N.M., Morel, F.M.M., 2005. Trace metal ion buffers and their use in culture studies. In: Andersen, R.A. (Ed.), Algal Culturing Techniques. Academic Press, Burlington.

Ting, C.S., Rocap, G., King, J., Chisholm, S.W., 2002. Cyanobacterial photosynthesis in the oceans: the origins and significance of divergent light-harvesting strategies. Trends in Microbiology, 10: 134-142.

Toledo, G., Palenik, B., Brahamsha, B., 1999. Swimming Marine Synechococcus Strains with Widely Different Photosynthetic Pigment Ratios Form a Monophyletic Group. Applied and Environmental Microbiology, 65: 5247-5251.

466 Twining, B.S. et al., 2003. Quantifying trace elements in individual aquatic protist cells with a
467 synchrotron X-ray fluorescence microprobe. Analytical Chemistry, 75: 3806-3816.
468
469 Twining, B.S., Baines, S.B., 2013. The trace metal composition of marine phytoplankton.
470 Annual Review of Marine Science, 5: 191-215.
471
472 Wozniak, B., Dera, J., 2007. Light Absorption in Sea Water. Atmospheric and oceanographic
473 sciences libary. Springer.
474
475 Zerkle, A.L., House, C.H., Brantley, S.L., 2005. Biogeochemical signatures through time as
476 inferred from whole microbial genomes. American Journal of Science, 305: 467-502.

Figure captions

two-column fitting image: **Fig. S.1.** The MARine Ecosystem DATa (MAREDAT; Buitenhuis et al., 2013) was used to find culturing conditions that avoid diffusion limitation despite variably-sized phytoplankton cells. The ratio of the Zn uptake rate over the maximum diffusion rate represents a measure of where growth starts to become diffusion limited, which is strongly dependent on the bioavailable Zn concentration (A). The percentage of the entire dataset that is not diffusion limited (solid line) for variable growth conditions (B-D), with the dashed line marking 2/3 of the total. Panels E-G investigate the boundary between diffusion-limitation (which occurs below the solid lines in all three panels) and its absence as a function of the ratio of surface area to biovolume (A/V). Even the largest diatom cultured here (horizontal dashed line) has an A/V ratio that lies in the non-diffusion-limited field for the chosen bioavailable Zn concentration (vertical red line in E) and would remain there for Zn/P ratios as high as 4 mmol mol^{-1}, or growth rates as high as 1.6 d^{-1}.

full page: **Fig. S.2.** Absorbance and fluorescence spectra of all four measured cyanobacteria strains. From left to right: *Prochlorococcus marinus* (CCMP 2389), and the three *Synechococcus sp.* CCMP 1183, CCMP 1334, and CCMP 2370.

single-column fitting image: **Fig. S.3.** Illustration of how cyanobacteria owe their vivid colors to the interplay between the absorbance spectra of photosynthetic pigments and the macromolecular structure of their light harvesting apparatus (phycobilisome).

two-column fitting image: **Fig. S.4.** The relationships between Fe and Zn use efficiencies and cellular metal quotas (A and B), their relationship to the quota of the other element (C and D), and a comparison between surface area normalized Zn uptake rates and element quotas relative to P (E and F). The dashed line is showing the global average Fe/P and Zn/P in oceanic phytoplankton from Twining and Baines (2013).

Zn isotope fractionation during uptake into marine phytoplankton: implications for oceanic zinc isotopes

Michael Köbberich[1*] and Derek Vance[1]

*To whom correspondence should be addressed

Submitted to: ***Chemical Geology***

Special issue: ***GEOTRACES - Goldschmidt Session 10i***

Corresponding author

Michael Köbberich, phone: +41 (0) 44 632 07 30, email: michael.koebberich@alumni.ethz.ch

Author affiliations

[1] Institute of Geochemistry and Petrology, Department of Earth Sciences, ETH Zurich, Clausiusstrasse 25, CH-8092 Zurich, Switzerland

Running head

Ligand controlled Zn isotope fractionation

Keywords

Zinc isotopes, Ligands, Phytoplankton culturing, Metal uptake, GEOTRACES, Trace Metals.

Abstract

The extreme scarcity of zinc (Zn) in the euphotic zone, coupled to deep enrichments, is consistent with biological uptake at the surface and regeneration at depth. In the context of a nutrient-type depth profile so clearly shaped by uptake into phytoplankton, the growing dataset for Zn isotopes presents a challenge. These data either show very minor isotope effects associated with extreme depletion, or enrichment of the light isotopes in the upper ocean. In contrast, culturing of eukaryotes in the laboratory suggests that light Zn isotopes are preferentially taken up into diatoms and coccoliths, implying that Zn depletion at the surface should be associated with extremely heavy residual dissolved signals.

Here we present the first Zn isotope measurements for cultured marine cyanobacteria and compare these data to those for eukaryotic diatoms grown under identical conditions. Of the four cyanobacteria cultured, belonging to the genera *Synechococcus* and *Prochlorococcus*, three preferentially take up light Zn into the cell, with a variability that is not fundamentally different between pro- and eukaryotic phytoplankton. We also observe only very subtle differences between Zn/P and Fe/P uptake ratios for these three cyanobacteria groups relative to diatoms grown under the same conditions. A fourth strain exhibits preferential uptake of heavy Zn isotopes, and very high Zn/P ratios. Overall, we speculate that the observed variability among cyanobacteria may be related to the molecular structure of their photosynthetic light harvesting apparatus, adapted to significantly different light niches.

These new and published culture data support the hypothesis that cellular δ^{66}Zn in culture might largely be controlled by the organic ligands that bind Zn in the medium. Given that the Zn-binding ligands in the ocean have thermodynamic stability constants that are orders of magnitude smaller than the EDTA used in culture media, the surprisingly subtle Zn isotope variability in some parts of the surface ocean may be reconciled with culture data by the lesser, near zero, preference of these weaker complexes for heavy Zn isotopes.

1. Introduction

Intracellular metal quotas (Twining and Baines, 2013; Twining et al., 2003) show that zinc (Zn) and iron (Fe) are the two most abundant trace metals in marine phytoplankton (Morel et al., 2014; Twining and Baines, 2013). Extremely low bioavailable Fe concentrations limit the fixation of atmospheric carbon dioxide (CO_2) by phytoplankton in about 30% of the global surface ocean (Moore et al., 2013), and likely also near the deep chlorophyll maximum of stratified subtropical mid-ocean gyres (Hopkinson and Barbeau, 2008; Sedwick et al., 2005; Sunda and Huntsman, 2015). Although the jury is still out on whether Zn co-limits phytoplankton growth in certain regions of the global ocean (*c.f.* Moore et al., 2013), Zn is often equally, if not more, abundant in the cell than Fe (Twining and Baines, 2013). Both metals serve as co-factors in enzymes of key metabolic pathways. Important examples of Zn containing enzymes are carbonic anhydrases, essential during biomass buildup from reduced carbon (C) and light (Domsic et al., 2008; Morel et al., 2014; Roberts et al., 1997), or alkaline phosphatases for the acquisition of organic phosphorus (P) when phosphate is scarce (Cox and Saito, 2013; Morel et al., 2014; Shaked et al., 2006). Superoxide dismutases can also require sizeable fractions of the cellular Fe and Zn pool, in particular in phototrophs, where light-induced reactions often come with toxic superoxide anions (O_2^-) that can be reduced by this enzyme (Morel, 2008; Wolfe-Simon et al., 2005). As a result, Zn is extremely scarce in the surface ocean, while the deep ocean is enriched, consistent with biological uptake in the euphotic zone and its regeneration at depth (Bruland, 1980; Bruland et al., 2014).

Metal stable isotope data, increasingly available through the international GEOTRACES program, provide a new way of investigating the impact of trace metal availability on phytoplankton growth. However, the data available to date for oceanic Zn isotopes have presented some challenging puzzles. For example, despite drawdown by diatom uptake during northward flow of surface waters, of close to 99% of the Zn upwelled in the Southern Ocean, the Zn-depleted residual water is not shifted to very heavy values (Wang et al., this volume; Zhao et al., 2014), as would be expected for preferential uptake of light isotopes into cells.

Furthermore, for nearly all regions outside the Southern Ocean (Conway and John, 2014; Conway and John, 2015; John et al., 2018), dissolved Zn in the upper ocean is significantly enriched in light Zn isotopes compared to the globally rather homogeneous deep ocean. Though Samanta et al. (2017) invoke the uptake of light isotopes with decreased Zn abundances in the surface Tasman Sea, the data are noisy, the correlation is very weak (r^2 = 0.21, MSWD = 15) and the fractionation factor implied is within uncertainty of zero. The same very weak relationship and near zero fractionation are seen in the data of Wang et al. (this volume). These findings seem to be at odds with the expectation that light isotopes would be preferentially taken up into cells, and with laboratory culture experiments that find the biomass of marine eukaryotic algae to be enriched in light Zn isotopes with respect to the experimental medium (John and Conway, 2014; John et al., 2007; Köbberich and Vance, 2017; Köbberich and Vance, 2018; Samanta et al., 2017).

Taxonomic differences among distinct groups of phytoplankton have been considered to drive some of the observed regional and global variability in Zn abundances in the ocean. For example, elevated Zn in diatoms (Twining and Baines, 2013) has been suggested to control Southern Ocean concentrations and, through the water masses advected from it, the pattern of variability in the global ocean (Vance et al., 2017). On the other hand, it is well-established that cellular Zn is closely related to its bioavailability in seawater (Sunda and Huntsman, 1992), leaving it unclear to what extent changes in the proteome are relevant (Cox and Saito, 2013; Twining and Baines, 2013). Beyond diatoms, Samanta et al. (2017) observed electron transport rates and the photosynthetic efficiency to increase with increasing free Zn^{2+} concentration in another eukaryote, *Emiliania huxleyi*, which was speculated to be due to increased carbonic anhydrase activity.

The global biogeography of phytoplankton is such that a great deal of the total chlorophyll belongs to only two major groups of phytoplankton, namely *Synechococcus* or *Prochlorococcus* (Follows and Dutkiewicz, 2010; Follows et al., 2007; Menemenlis et al., 2005). Furthermore, these prokaryotic cyanobacteria are direct descendants of the earliest

oxygenic phototrophs, originating during a period of Earth history distinctly different in its ocean chemistry (Falkowski and Knoll, 2007; Knoll et al., 2012; Saito et al., 2003; Sunda and Huntsman, 2015). It has been suggested that this resulted in elevated minimum Fe requirements in prokaryotes, and that this explains their high requirement for Fe relative to eukaryotes in the modern ocean (Brand, 1991; Österberg, 1974; Saito et al., 2003; Sunda and Huntsman, 2015).

In the light of these considerations, constraints on how cyanobacteria take up Zn and its isotopes are required. Here we address this requirement. We also present new data for diatoms, cultured under conditions that are as close as possible to those for the cyanobacteria. Our aim is to explore the relative importance of species-dependent differences versus environmental controls for trace metal systematics versus, with implications for the evolution of trace metal requirements in an ocean in which the biology and chemistry have both changed through time. Finally, we consider the emerging dataset for oceanic Zn isotopes in the context of these new constraints, as well as published data, from culture experiments.

2. Materials & Methods

Culturing media were prepared either from salts that were of trace metal purity, or from solutions that were cleaned using a chelating resin (Chelex® 100, Bio-Rad, USA). All ultrapure water came from a Milli-Q® integral water purification system (Merck, Millipore, Germany) with a conductivity of 18.2 MΩ·cm. Reagent grade acids used for preparative purposes were twice purified by sub-boiling distillation before use (DST-1000, Savillex, USA). Handling of all samples and reagents was carried out under "Class 100" clean laboratory conditions at constant humidity of around 10 %, and a temperature of 21.2 ± 0.2 °C.

2.1 Phytoplankton strains

Three different diatoms and four distinct cyanobacteria strains, all axenic, were obtained from the National Center for Marine Algae and Microbiota (NCMA), formerly known as Provasoli-Guillard Center for Culture of Marine Phytoplankton (CCMP), Bigelow Laboratories, USA.

Two of the chosen diatoms, *Chaetoceros sp.* (CCMP 199) and *Thalassiosira oceanica* (CCMP 1005), originate from oligotrophic surface waters of the Sargasso Sea, North Atlantic. The third, *Thalassiosira weissflogii* (CCMP 1336) came from coastal waters of Long Island Sound, North Atlantic, USA. Three representatives of the genus *Synechococcus* (CCMP 1183, 1334, and 2370, the latter two are also known as WH 7803 and 8102) and *Prochlorococcus marinus* (CCMP 2389, *a.k.a.* MED 4) were chosen to represent the prokaryotic phylum of cyanobacteria. All four prokaryotes are open ocean strains, two of which (CCMP 1334 and 2370) originate in the oligotrophic surface waters of the Sargasso Sea, North Atlantic. Sterile techniques were used whenever cultures or media solutions were handled. Axenic conditions were monitored by inspecting small aliquots of stained culture solutions by microscopic methods.

An important aim of this contribution is to explore inter-species Zn isotope effects associated with Zn uptake into the cell. Biological fractionation of Zn isotopes during uptake has been related to active transport across the cell membrane (John et al., 2007), a mechanism that for Fe has been shown to be a surface-area related process (Sunda and Huntsman, 1995; Sunda and Huntsman, 1997). The set of species chosen here span the entire size range of pico- and nano-phytoplankton and differ in their surface area to biovolume (A/V) ratio as calculated from their cellular geometry (Fig. 1). The cellular dimensions and geometries of 1362 diatoms (Leblanc et al., 2012) and 181 coccolithophores (O'Brien et al., 2013) came from the MARine Ecosystem DATa (MAREDAT; Buitenhuis et al., 2013) project. Geometric models that are used for calculating cell surface areas and biovolumes (Leblanc et al., 2012; Sun and Liu, 2003) can also be linked to empirical carbon (C) biomass estimates (Leblanc et al., 2012; Smayda, 1978). We use this information to compare our laboratory cultures with the A/V ratios that have previously been considered relevant to natural environments (Fig. 1).

2.2 Culturing techniques

The culturing conditions were similar to Köbberich and Vance (2017). A short summary is given below with the most important differences highlighted. Light was supplied to all

phytoplankton cultures in 15- to 9-hour day to night cycles. A constant photon flux density of 50 rather than 40 μmol m^{-2} s^{-1} was used, with one important exception: the high light adapted *Prochlorococcus* strain CCMP 2389 was maintained at 25 μmol m^{-2} s^{-1}, as verified with a newly calibrated spherical quantum sensor LI-193 (LI-COR®, Nebraska, USA). Cell numbers for calculating specific growth rates were obtained by Coulter counting on a daily basis or by using a hemocytometer, as described in Köbberich and Vance (2017).

The artificial culture medium, used here to allow comparison across a range of different eukaryotic and prokaryotic phytoplankton organisms at similar bioavailable Zn^{2+} levels, is similar to that previously reported in Köbberich and Vance (2017). This medium has a seawater base adjusted to a final salinity of about 36 g kg^{-1}. Total ethylenediaminetetraacetic acid (EDTA) concentrations were in the range 95 - 97 μmol l^{-1}, and Zn was kept constant to allow inter-species comparison at identical bioavailable Zn. Total Zn concentrations were thus adjusted to obtain free divalent Zn^{2+} and inorganically bound Zn (Zn′) levels in the range 67 - 72 and 100 - 109 pmol l^{-1}, respectively, for all eukaryotes and *Synechococcus* strains. Aqueous Zn speciation has been calculated following the recommendations of Sunda et al. (2005) and references therein. The artificial seawater medium used to culture the *Prochlorococcus* strain CCMP 2389 had to differ from that used for all other strains for two distinct, though related, reasons. Firstly, *P. marinus* simply does not grow in the above-described broad-spectrum medium. Secondly, to our knowledge, there is currently no recipe available that maintains *Prochlorococcus* as well as all the other species of interest. We thus designed a newly developed medium that mimics the above-described solution as closely as possible, while still achieving sufficient *Prochlorococcus* growth (see Supplementary Information S.1 for further details).

All phytoplankton cells were harvested, *i.e.* separated from their residual culturing medium, at or shortly after mid exponential growth, with 0.2 μm filters, using pre-cleaned vertical twin membrane centrifugal concentrators (Vivaspin 20, Sartorius, Germany). Shortly after harvesting, residual media remnants were removed by washing the collected cells with UV-

treated equatorial Atlantic seawater, with notably low Zn in the range of 0.01 - 0.05 nmol kg^{-1} (Zhao, 2011). The biomass collected on the filter was re-suspended in pre-cleaned NaCl of seawater osmolality, before the resulting cell suspension was pipetted out of the centrifugal concentrator. After evaporation to dryness, all samples were digested in double distilled 65% HNO_3 at 120 °C for ~16 hours. After a final dry-down, all digested samples were re-dissolved in 2 % HNO_3 for elemental analysis, followed by column chromatography and Zn isotopic analysis (see next section).

2.3 Elemental and stable isotope analysis

The procedures used for elemental and stable isotope analysis are identical to those previously described in Köbberich and Vance (2017) and very similar to those in previous publications from this laboratory (*e.g.*, Little et al., 2016; Vance et al., 2016a; Vance et al., 2016b). In brief, elemental analyses were done on a ThermoScientific Element XR™ inductively-coupled plasma mass spectrometer (ICP-MS). All samples for isotope analysis were purified by anion exchange chromatography (Archer and Vance, 2004; Bermin et al., 2006; Maréchal et al., 1999) and were measured on a Neptune Plus™ multiple-collector inductively-coupled plasma mass spectrometer (MC-ICP-MS) of the same manufacturer. Instrumental mass fractionation, or that occurring during ion exchange chromatography, was corrected using the double spike approach as described by Bermin et al. (2006) and Zhao et al. (2014), in combination with a data reduction scheme presented by Siebert et al. (2001). Procedural blanks were estimated by isotope dilution analysis and are negligible.

The data presented here are given in the standard delta notation, in per mil, reported relative to JMC 3-0749 (Maréchal et al., 1999): $\delta^{66}Zn\ (‰) = [(^{66}Zn/^{64}Zn)_{sample} / (^{66}Zn/^{64}Zn)_{JMC\text{-}Lyon}] - 1$. Accuracy and precision were monitored relative to a secondary standard, IRMM-3702, previously reported to yield a value of +0.32 ‰ (Cloquet et al., 2008; Ponzevera et al., 2006). Relative to JMC-Lyon, we obtain $\delta^{66}Zn = 0.30 \pm 0.06$ ‰ (2 SD, n = 163 over 380 days). All our culturing results are reported as the fractionation observed between the medium and the separated biomass, here denoted $\Delta^{66}Zn\ (‰) = \delta^{66}Zn_{biomass} - \delta^{66}Zn_{medium}$. Culture experiments

were only considered relevant for reporting when nearly 100% of the Zn initially added to the medium was recovered in the residual medium plus the biomass fraction after the experiment, as quantified by isotope dilution. All diagrams plot the external precision, based on replicate analyses of IRMM-3702 as noted above, unless internal errors exceed the external reproducibility.

3. Results

Based on measured growth and metal uptake data, the largest cultured diatom, *T. weissfloggi*, reached Zn uptake rates up to about 26% of the maximum that could be supplied to the cell by diffusion (Table 1). The prokaryotic organisms cultured here were much less likely to be diffusion limited - and consistently contained less than 1% of the amount of Zn that could be supplied by diffusion. Fe exerts a key control on phytoplankton growth and thus metal uptake (Köbberich and Vance, 2017; Sunda and Huntsman, 1995; Sunda and Huntsman, 1997), so that Table 1 also provides data supporting the suggestion that growth it not suppressed as a consequence of diffusion limited Fe supply.

Three different diatom strains, each grown on nitrate and urea as the sole N source, were generally found to grow fast, with specific growth rates between 0.65 and 0.77 d^{-1}. At identical irradiance and nutrient levels, three representatives of the genus *Synechococcus* grew at more variable rates, ranging from 0.42 to 0.82 d^{-1} (Fig. 2A). *Prochlorococcus marinus* – the smallest strain cultured here – grew at a specific growth rate of 0.28 d^{-1}, at half the irradiance level (25 µmol m^{-2} s^{-1}) applied to all other strains (50 µmol m^{-2} s^{-1}).

Fe uptake into marine phytoplankton has previously been shown to be a surface area related process (Sunda and Huntsman, 1995; Sunda and Huntsman, 1997). Surface area normalized Fe and Zn uptake rates, calculated from measured cellular quotas and the surface areas shown in Fig. 1, are high and variable for diatoms, reaching up to values that are often greater than 100 nmol m^{-2} d^{-1}. Those of prokaryotes are mostly much lower (Fig. 2B and C).

Carbon or P-normalized cellular Fe and Zn of all measured diatoms are in good agreement with previous culture work (Sunda and Huntsman, 1992; Sunda and Huntsman, 1995) at similar bioavailable metal concentrations. Measured metal to P quotas were converted to Zn/C assuming a Redfield stoichiometry of C:P of 106:1. In good agreement with previous work on a coastal *Synechococcus bacillaris* strain (Sunda and Huntsman, 2015), all studied cyanobacteria yielded higher cellular Fe quotas than the majority of cultured diatoms (Fig. 3A), while their absolute rates of metal transport across the cell membrane were generally found to be very low (Fig. 2B). Except for the *Synechococcus* strain CCMP 2370, the opposite was found for cellular Zn quotas (Fig. 3B), also at comparatively low uptake rates (Fig. 2C). This becomes most apparent if cellular Zn quotas are plotted as a function of Fe quotas (Fig. 3C). Excluding CCMP 2370, the highest Zn/P quotas of ~2 mmol mol^{-1} were found with low Fe/P ratios, while the lowest of ~0.5 mmol mol^{-1} were reached at Fe/P ~7 mmol mol^{-1}.

All the isotope results are given in Table 1. The biomass of the marine diatom *T. oceanica* shows a preference for light isotopes by 0.28‰, similar that previously observed for this strain for a comparable culture medium (Δ^{66}Zn; John et al., 2007; Köbberich and Vance, 2017).

4. Discussion

Of the two groups of organisms cultured here for Zn isotopes, the data for cyanobacteria are the most novel. Previous studies have presented data for diatoms (John et al., 2007; Köbberich and Vance, 2017; Köbberich and Vance, 2018), while Samanta et al. (2017) have published Zn isotope data for another eukaryote group, the coccoliths. Thus, we first discuss the variation within the cyanobacteria strains cultured, before moving on to compare these new data with the new and published data for eukaryotes.

4.1 Variations in metal uptake characteristics among cyanobacteria

Three of the four cyanobacteria cultured were found to have similar cellular Zn quotas to diatoms, though at the lower end of the latter's range. The opposite is true for cellular Fe quotas (Fig. 3A and 3B), a finding which is in agreement with previous work (Saito et al., 2003; Sunda

and Huntsman, 2015; Sunda and Huntsman, 1995). It is also obvious from Fig. 3, that CCMP 2370 differs from the other cyanobacteria in its Zn quota. Though this difference is less marked for Fe, it is also the case that the Fe quotas found for CCMP 2370 represent the higher end of the observed spectrum (Fig. 3C). High biomass associated Fe contents might indicate the presence of surface-bound Fe-hydroxides, which could adsorb large quantities of Zn, and this theory might be supported by positive biomass Δ^{66}Zn values (see Table 1 and Section 4.3; Gélabert et al., 2006; John et al., 2007). However, the variability in the overall cyanobacterial dataset, for both Fe- and Zn-quotas and including the data for CCMP 2370, is no greater than that seen in natural communities using X-ray fluorescence imaging techniques (Twining and Baines, 2013). Moreover, Tang and Morel (2006) did not detect any increase in cellular Zn/P at the total medium Fe concentrations used here, or for the biomass Fe/P ratios measured here. It is also the case that CCMP 2370 differs from all other cyanobacteria in the greater proportion of phycourobilin (PUB) in its total budget of chromophores (Six et al., 2007). There is, however, currently no known Zn containing enzyme involved in the biosynthesis of PUB. Whether the cellular Zn content could be related to such biochemical pathways remains to be addressed in future research (for additional thoughts see section S.5 of the Supplementary Information).

4.2 Similarities and differences between prokaryotic and eukaryotic metal uptake

Culture experiments are performed in a controlled environment. An assessment of taxonomic differences from such experiments is often only possible in terms of whether the phytoplankton of interest is well adapted to the culture conditions used, coupled to a comparison between those culturing conditions and the organism's natural habitat. Thus, despite an extensive body of literature on the physiological response to various types of environmental stress (for a review see Morel et al., 2014) applied in laboratory cultures, it remains challenging to separate purely taxonomic effects from imposed environmental factors.

The precise culture conditions chosen here for the eukaryotic organisms were adjusted to yield similar specific growth rates for each organism, using published constraints (Sunda and

Huntsman, 1995; Sunda and Huntsman, 1997). Thus, though the open ocean diatom *T. oceanica*, as well as a representative of the genus *Chaetoceros*, grew at similar rates for the same Fe′, the same growth rates were only achieved for the coastal species, *T. weissflogii*, at Fe′ that was almost twice as high (Table 1). Prokaryotes such as the tiny *Prochlorococcus* simply behave too differently to reasonably expect them to yield the same fast growth rates as diatoms in culture (*c.f.* Supplementary Information S.1). In our experiments, CCMP 1183 and 2370 were at least close, though somewhat more variable (Fig. 2A).

4.3 Ligand control on Δ^{66}Zn recorded in phytoplankton

Based on precautions to avoid diffusion-limited Zn transport towards the cell surface (*c.f.* section S.2 in the Supplementary Information), we can essentially exclude the possibility that any of the negative Δ^{66}Zn observed here are likely to be caused by the slightly faster diffusion rates of the lighter ^{64}Zn isotope. Only the cyanobacteria strain CCMP 2370, with unusually high cellular Zn quotas, was found to yield positive Δ^{66}Zn values with respect to the bulk culture medium (Fig. 4). All other phytoplankton, whether pro- or eukaryotic, consistently yielded negative Δ^{66}Zn values (Table 1). These findings are in good agreement with previous culture experiments (John et al., 2007; Köbberich and Vance, 2017; Samanta et al., 2017), at similar bioavailable Zn levels, as illustrated in Fig. 5.

The equilibrium fractionation between Zn-EDTA and 'free' Zn is such that heavy Zn isotopes are preferentially bound to the organic chelator (Ban et al., 2002; Ding et al., 2010a; Ding et al., 2010b; Markovic et al., 2017), while the bioavailable Zn^{2+} pool is enriched in light Zn isotopes - before any interaction with phytoplankton. In agreement with the suggestion of John et al. (2007), we thus argue that a substantial portion of the observed Δ^{66}Zn in cultured phytoplankton is actually the result of this equilibrium fractionation in the medium, rather than resulting from biological uptake. Although there is strain-dependent variability in the extent to which the light Zn isotope is taken up into phytoplankton, there are no systematic differences between cyanobacteria and diatoms. In fact, excluding CCMP 2370, the absolute ranges observed among different representatives of both clades are almost indistinguishable from each

other. Neither absolute rates of Zn transport across the cell surface area, nor A/V ratios (see Supplementary Information, Fig. S.1), seem to correlate with the extent to which light Zn isotopes are preferentially taken up. This could simply be due to the fact that the studied diversity is still too small, obscuring any potential pattern. On the other hand, the uptake mechanism may be important, given that there is an increasing preference for light Zn isotopes as a result of additional active transport across the cell wall beyond the level associated with high-affinity transporters alone (John et al., 2007). Thus, the observed variability might be caused by the fact that the onset of low-affinity Zn uptake may occur at different bioavailable Zn concentrations, as previously identified for *T. oceanica* (John et al., 2007) and *Emiliania huxleyi* (Samanta et al., 2017). In this study, bioavailable Zn was chosen to be at the higher end of the range previously considered relevant for high-affinity uptake (for a more detailed discussion, see Köbberich and Vance, 2017). Thus, it is possible that light signatures seen in some of the strains studied here might be explained by isotope fractionation associated with active low-affinity transporters superimposed on a fractionation caused by the high-affinity mechanism.

5. Conclusion and oceanic implications

The two first order features of the oceanic distributions of Zn isotopes that are emerging as data accumulates are: 1) in the Southern Ocean, despite often dramatic drawdown of Zn at the surface, mostly by diatoms, variations in the small residual Zn pool are very muted (*e.g.*, Wang et al., this volume; Zhao et al., 2014); 2) outside the Southern Ocean, residual seawater tends to be lighter in the upper ocean, seeming to imply the uptake of heavy isotopes (*e.g.*, Conway and John, 2014), though where high depth resolution is available near the surface it is often the case that these light values actually occur in the immediate sub-surface (*e.g.*, Wang et al., this volume). Though variations in dissolved Zn isotopes in the surface Southern Ocean are indeed muted, there is also a slight minimum at 100-200m (Wang et al., this volume). The above observations are both, at first glance, inconsistent with the finding of light Zn isotopes in

phytoplankton cells in culture. Here we discuss each of the above observations of the real ocean in turn, in the context of the summary of culturing experiments in Fig. 5.

An important conclusion from Fig. 5 is that a large proportion of the enrichment of light Zn in a variety of studied pro- and eukaryotic phytoplankton can be explained by the presence of organic ligands in culture media. Consistent with a postulate by John et al. (2007), heavy Zn isotopes are preferentially bound to the trace metal buffer EDTA in culture media, while the 'free' bioavailable Zn pool is already enriched in light isotopes before uptake. A significant proportion of light Zn found in phytoplankton after a culture experiment might thus be the result of an aqueous equilibrium in seawater, rather than the consequence of kinetic isotope fractionation during active transport across the cell wall. Although the uncertainty on the isotope fractionation associated with the relevant Zn-EDTA equilibrium is still large (Ban et al., 2002; Ding et al., 2010a; Ding et al., 2010b; Markovic et al., 2017), kinetic isotope effects associated with uptake are only rarely outside the range that could be explained by the presence of this strong ligand.

One could argue that, since the real ocean also contains strong ligands that bind Zn, it is still the Δ^{66}Zn fractionation with respect to bulk medium that is the most relevant for the great majority of oceanic regimes. For example, Ellwood and Van den Berg (2000) have shown that 94 - 99% of all Zn in the open NE Atlantic is bound to strong organic complexes. Free Zn concentrations - at 6 - 20 pmol l^{-1} - in those regions are low, but not low enough to limit the growth of a typical oceanic species (Ellwood and Van den Berg, 2000). Thus, the situation regarding complexation of Zn in the real ocean is *qualitatively* analogous to that in culture experiments, with the bioavailable pool being lighter than the ligand bound fraction.

In the surface Southern Ocean, Zn is rapidly drawn down by diatom uptake, by almost 2 orders of magnitude relative to the upwelled deep waters (*e.g.*, Vance et al., 2017; Zhao et al., 2014). If such uptake prefers the light isotope to the extent seen for $\Delta^{66}Zn_{\text{biomass - bulk medium}}$ in culturing experiments (Fig. 5), then the δ^{66}Zn of the residual Zn-depleted water should exceed 1‰, when in fact it barely rises above the deep ocean average δ^{66}Zn of +0.5‰ more than analytical

uncertainty (Wang et al., this volume; Zhao et al., 2014). It could be that the answer to this problem originates with differences in the speciation of Zn in culture versus seawater. Markovic et al. (2017) present experimental findings showing that isotope fractionation between free Zn and the organically-bound complex depends on the thermodynamic stability constant for that complex, which for EDTA is about 6 orders of magnitude greater than those for Zn in the real ocean (*e.g.*, Bruland, 1989; Ellwood and van den Berg, 2000; Markovic et al., 2017). However, Bruland (1989) also showed that the *conditional* stability constant for Zn-EDTA complexes in seawater are lower than those for natural organic ligands, due to side reactions between EDTA and Ca and Mg ions that do not occur for the natural ligands (Bruland et al., 1989).

Finally, we turn to the apparently light Zn isotope values in areas outside the Southern Ocean. John and Conway (2014) have suggested an explanation in terms of preferential loss of heavy isotope through scavenging to particulate organic matter. One issue with this suggestion is that the experiment in which scavenging, and Zn isotope fractionation associated with it, was observed (John and Conway, 2014) contained none of the organic ligands that stabilize Zn in solution, whereas most of the surface ocean contains more than 10 times more Zn-specific ligands than total dissolved Zn found in the NE Atlantic (Ellwood and Van den Berg, 2000). The one part of the surface ocean where this is known not to be the case is the Southern Ocean, (Baars and Croot, 2011), and this is where heavy surface isotopes are not seen.

As shown in the data compilation in Wang et al. (this volume), most profiles with generally negative δ^{66}Zn in the upper ocean actually feature a heavy value right at the surface. In at least some cases, this upward move to heavy Zn isotopes is defined by more than a single sample. We suggest, therefore, that the data are often consistent with uptake of slightly light isotopes at the surface and that the light isotopes that apparently dominate the upper ocean in *e.g.* the North Atlantic (Conway and John, 2014) are at least partially the result of very shallow sub-surface (peaking at about 100 m but extending down to 500 m) regeneration of biomass-associated light Zn isotopes (*e.g.*, Bermin et al., 2006). It is also clear, however, that mass

balance considerations mean that such a process cannot explain the overall light upper layer outside the Southern Ocean - *i.e.* the upper 500m. This Southern Ocean biogeochemical divide is emerging as a key feature of the ocean biogeochemistry of Zn, consistent with the behavior of other nutrients in the ocean (*e.g.*, Marinov et al., 2006; Sarmiento et al., 2004; Vance et al., 2017). The Zn-rich deep cycle is fed by deep waters that only re-connect to the surface in the Southern Ocean, and sits below a rather isolated extra-Southern shallow ocean exhibiting different processes. Recent studies have highlighted a very similar pattern for Cd and its isotopes, with Cd isotopes apparently buffered to a surprisingly constant value in this low-latitude surface pool (*e.g.*, Xie et al., 2017; Sieber et al., this volume). It is speculation at present, but the idea that one of the processes that have been invoked for Cd, supply from the atmosphere (Xie et al., 2017), could also explain light Zn in the low latitude surface merits further investigation.

Acknowledgements

We are grateful to Alysia D. Cox for help with setting up a phytoplankton culturing lab at ETH Zurich and to Timothy I. Eglinton for allowing us access to biology laboratories and incubator facilities. We also wish to thank Corey Archer for valuable support with elemental and isotopic analysis and Amélie Ritscher for her work as a research assistant at ETH Zurich. Financial support was provided by ETH and the Swiss National Science Foundation (SNF) through grant 200021-143262.

References

Archer, C., Vance, D., 2004. Mass discrimination correction in multiple-collector plasma source mass spectrometry: an example using Cu and Zn isotopes. Journal of Analytical Atomic Spectrometry, 19: 656-665.

Baars, O., Croot, P.L., 2011. The speciation of dissolved zinc in the Atlantic sector of the Southern Ocean. Deep Sea Research Part II: Topical Studies in Oceanography, 58: 2720-2732.

Ban, Y., Aida, M., Nomura, M., Fujii, Y., 2002. Zinc isotope separation by ligand exchange chromatography using cation exchange resin. Journal of Ion Exchange, 13: 46-52.

Bermin, J., Vance, D., Archer, C., Statham, P.J., 2006. The determination of the isotopic composition of Cu and Zn in seawater. Chemical Geology, 226: 280-297.

Brand, L.E., 1991. Minimum iron requirements of marine phytoplankton and the implications for the biogeochemical control of new production. Limnology and Oceanography, 36: 1756-1771.

Bruland, K.W., 1980. Oceanographic distributions of cadmium, zinc, nickel, and copper in the North Pacific Earth and Planetary Science Letters, 47: 176-198.

Bruland, K.W. (1989) Complexation of zinc by natural organic ligands in the central North Pacific. Limnology and Oceanography 34: 269-285.

Bruland, K.W., Middag, R., Lohan, M.C., 2014. Controls of trace metals in seawater. In: Heinrich, D.H., Karl, K.T. (Eds.), Treatise on Geochemistry. Elsevier, Oxford, pp. 19-51.

Buitenhuis, E.T. et al., 2013. MAREDAT: towards a world atlas of MARine Ecosystem DATa. Earth System Science Data, 5: 227-239.

Cloquet, C., Carignan, J., Lehmann, M., Vanhaecke, F., 2008. Variation in the isotopic composition of zinc in the natural environment and the use of zinc isotopes in biogeosciences: a review. Analytical and Bioanalytical Chemistry, 390: 451-463.

Conway, T.M., John, S.G., 2014. The biogeochemical cycling of zinc and zinc isotopes in the North Atlantic Ocean. Global Biogeochemical Cycles, 28: 1111-1128.

Conway, T.M., John, S.G., 2015. The cycling of iron, zinc and cadmium in the North East Pacific Ocean – insights from stable isotopes. Geochimica et Cosmochimica Acta, 164: 262-283.

Cox, A.D., Saito, M.A., 2013. Proteomic responses of oceanic *Synechococcus* WH8102 to phosphate and zinc scarcity and cadmium additions. Frontiers in Microbiology, 4: 387, pp. 1-17.

Ding, X., Nomura, M., Fujii, Y., 2010a. Zinc isotope effects by chromatographic chelating exchange resin. Progress in Nuclear Energy, 52: 164-167.

Ding, X., Nomura, M., Suzuki, T., Fujii, Y., 2010b. Chromatographic zinc isotope separation by chelating exchange resin. Chromatographia, 71: 195-199.

Domsic, J.F. et al., 2008. Entrapment of Carbon Dioxide in the Active Site of Carbonic Anhydrase II. Journal of Biological Chemistry, 283: 30766-30771.

Ellwood, M.J., Van den Berg, C.M.G., 2000. Zinc speciation in the Northeastern Atlantic Ocean. Marine Chemistry, 68: 295-306.

Falkowski, P.G., Knoll, A.H., 2007. Evolution of primary producers in the sea. Elsevier Academic Press.

Follows, M.J., Dutkiewicz, S., Grant, S., Chisholm, S.W., 2007. Emergent Biogeography of Microbial Communities in a Model Ocean. Science, 315: 1843-1846.

Follows, M.J., Dutkiewicz, S., 2010. Modeling Diverse Communities of Marine Microbes. Annual Review of Marine Science, 3: 427-451.

Gélabert, A. et al., 2006. Interaction between zinc and freshwater and marine diatom species: surface complexation and Zn isotope fractionation. Geochimica et Cosmochimica Acta, 70: 839-857.

Hopkinson, B.M., Barbeau, K.A., 2008. Interactive influences of iron and light limitation on phytoplankton at subsurface chlorophyll maxima in the eastern North Pacific. Limnology and Oceanography, 53: 1303-1318.

John, S.G., Geis, R.W., Saito, M.A., Boyle, E.A., 2007. Zinc isotope fractionation during high-affinity and low-affinity zinc transport by the marine diatom *Thalassiosira oceanica*. Limnology and Oceanography, 52: 2710-2714.

John, S.G., Conway, T.M., 2014. A role for scavenging in the marine biogeochemical cycling of zinc and zinc isotopes. Earth and Planetary Science Letters, 394: 159-167.

John, S.G., Helgoe, J., Townsend, E., 2018. Biogeochemical cycling of Zn and Cd and their stable isotopes in the Eastern Tropical South Pacific. Marine Chemistry 201: 256-262.

Knoll, A.H., Canfield, D.E., Konhauser, K.O. (Eds.), 2012. Fundamentals of Geobiology. John Wiley & Sons, Ltd., pp. 443.

Köbberich, M., Vance, D., 2017. Kinetic control on Zn isotope signatures recorded in marine diatoms. Geochimica et Cosmochimica Acta, 210: 97-113.

Köbberich, M., Vance, D., 2018. Zinc association with surface-bound iron-hydroxides on cultured marine diatoms: A zinc stable isotope perspective. Marine Chemistry.

Leblanc, K. et al., 2012. A global diatom database – abundance, biovolume and biomass in the world ocean. Earth System Science Data, 4: 149-165.

Little, S.H., Vance, D., McManus, J., Severmann, S., 2016. Key role of continental margin sediments in the oceanic mass balance of Zn and Zn isotopes. Geology, 44: 207-210.

Maréchal, C.N., Télouk, P., Albarède, F., 1999. Precise analysis of copper and zinc isotopic compositions by plasma-source mass spectrometry. Chemical Geology, 156: 251-273.

Marinov, I., Gnanadesikan, A., Toggweiler, J.R., Sarmiento, J.L., 2006. The Southern Ocean biogeochemical divide. Nature, 441: 964-967.

Markovic, T. et al., 2017. Experimental determination of zinc isotope fractionation in complexes with the phytosiderophore 2'-deoxymugeneic acid (DMA) and its structural analogues, and implications for plant uptake mechanisms. Environmental Science & Technology, 51: 98–107.

Menemenlis, D. et al., 2005. NASA supercomputer improves prospects for ocean climate research. Eos, Transactions American Geophysical Union, 86: 89-96.

Moore, C.M. et al., 2013. Processes and patterns of oceanic nutrient limitation. Nature Geoscience, 6: 701-710.

Morel, F.M.M., 2008. The co-evolution of phytoplankton and trace element cycles in the oceans. Geobiology, 6: 318-324.

Morel, F.M.M., Milligan, A.J., Saito, M.A., 2014. Marine bioinorganic chemistry: the role of trace metals in the oceanic cycles of major nutrients. In: Heinrich, D.H., Karl, K.T. (Eds.), Treatise on Geochemistry. Elsevier, Oxford, pp. 123-150.

O'Brien, C.J. et al., 2013. Global marine plankton functional type biomass distributions: coccolithophores. Earth System Science Data, 5: 259-276.

Österberg, R., 1974. Origins of metal ions in biology. Nature, 249: 382-383.

Ponzevera, E. et al., 2006. Mass discrimination during MC-ICPMS isotopic ratio measurements: investigation by means of synthetic isotopic mixtures (IRMM-007 series) and application to the calibration of natural-like zinc materials (Including IRMM-3702 and IRMM-651). Journal of the American Society for Mass Spectrometry, 17: 1413-1428.

Roberts, S.B., Lane, T.W., Morel, F.M.M., 1997. Carbonic anhydrase in the marine diatom *Thalassiosira weissflogii* (Bacillariophyceae). Journal of Phycology, 33: 845-850.

Saito, M.A., Sigman, D.M., Morel, F.M.M., 2003. The bioinorganic chemistry of the ancient ocean: the co-evolution of cyanobacterial metal requirements and biogeochemical cycles at the Archean–Proterozoic boundary? Inorganica Chimica Acta, 356: 308-318.

Samanta, M., Ellwood, M.J., Sinoir M., Hassler C.S., 2017. Dissolved zinc isotope cycling in the Tasman Sea, SW Pacific Ocean. Marine Chemistry: 192: 1-12.

Samanta, M., Ellwood, M.J., Strzepek, R.F., 2017. Zinc isotope fractionation by *Emiliania huxleyi* cultured across a range of free zinc ion concentrations. Limnology and Oceanography: 63: 660-671.

Sarmiento, J.L., Gruber, N., Brzezinski, M.A., Dunne, J.P., 2004. High-latitude controls of thermocline nutrients and low latitude biological productivity. Nature, 427: 56-60.

Sedwick, P.N., Church, T.M., Bowie, A.R., Marsay, C.M., Ussher, S.J., Achilles, K.M., Lethaby, P.J., Johnson, R.J., Sarin, M.M., McGillicuddy, D.J. (2005), Iron in the Sargasso Sea (Bermuda Atlantic Time- series Study region) during summer: Eolian imprint, spatiotemporal variability, and ecological implications, Global Biogeochemical Cycles, 19, GB4006.

Shaked, Y., Xu, Y., Leblanc, K., Morel, F.M.M., 2006. Zinc availability and alkaline phosphatase activity in Emiliania huxleyi: Implications for Zn-P co-limitation in the ocean. Limnology and Oceanography, 51: 299-309.

Sieber, M., Conway, T.M., de Souza, G.F., Obata, H., Takano, S., Sohrin, Y., Vance, D., in press. Physical and biogeochemical controls on the distribution of dissolved cadmium and its isotopes in the Southwest Pacific Ocean. Chemical Geology, this volume.

Siebert, C., Nägler, T.F., Kramers, J.D., 2001. Determination of molybdenum isotope fractionation by double-spike multicollector inductively coupled plasma mass spectrometry. Geochemistry, Geophysics, Geosystems, 2: 1032.

Six, C. et al., 2007. Diversity and evolution of phycobilisomes in marine *Synechococcus spp.*: a comparative genomics study. Genome Biology, 8: R259 pp. 1-22.

Smayda, T.J., 1978. From phytoplankters to biomass. In: Sournia, A. (Ed.), Phytoplankton manual. Museum National d'Histoire Naturelle, Paris, pp. 273-279.

Sun, J., Liu, D., 2003. Geometric models for calculating cell biovolume and surface area for phytoplankton. Journal of Plankton Research, 25: 1331-1346.

Sunda, W.G., Huntsman, S.A., 1992. Feedback interactions between zinc and phytoplankton in seawater. Limnology and Oceanography, 37: 25-40.

Sunda, W.G., Huntsman, S.A., 1995. Iron uptake and growth limitation in oceanic and coastal phytoplankton. Marine Chemistry, 50: 189-206.

Sunda, W.G., Huntsman, S.A., 1997. Interrelated influence of iron, light and cell size on marine phytoplankton growth. Nature, 390: 389-392.

Sunda, W.G., Price, N.M., Morel, F.M.M., 2005. Trace metal ion buffers and their use in culture studies. In: Andersen, R.A. (Ed.), Algal Culturing Techniques. Academic Press, Burlington.

Sunda, W., Huntsman, S., 2015. High iron requirement for growth, photosynthesis, and low-light acclimation in the coastal cyanobacterium *Synechococcus bacillaris*. Frontiers in Microbiology, 6: 561.

Tang, D., Morel, F.M.M., 2006. Distinguishing between cellular and Fe-oxide-associated trace elements in phytoplankton. Marine Chemistry, 98: 18-30.

Twining, B.S. et al., 2003. Quantifying trace elements in individual aquatic protist cells with a synchrotron X-ray fluorescence microprobe. Analytical Chemistry, 75: 3806-3816.

Twining, B.S., Baines, S.B., 2013. The trace metal composition of marine phytoplankton. Annual Review of Marine Science, 5: 191-215.

Vance, D. et al., 2016a. The oceanic budgets of nickel and zinc isotopes: the importance of sulfidic environments as illustrated by the Black Sea. Philosophical Transactions of the Royal Society A: Mathematical, Physical and Engineering Sciences, 374: 1-26.

Vance, D. et al., 2016b. The behaviour of Cu and Zn isotopes during soil development: controls on the dissolved load of rivers. Chemical Geology, 445: 36-53.

Vance, D. et al., 2017. Silicon and zinc biogeochemical cycles coupled through the Southern Ocean. Nature Geoscience, 10: 202-206.

Wang, R.M., Archer, C., Bowie, A.R., Vance, D., in press. Zinc and nickel isotopes in seawater from the Indian Sector of the Southern Ocean: the impact of natural iron fertilization versus Southern Ocean hydrography and biogeochemistry. Chemical Geology, this volume.

Wolfe-Simon, F., Grzebyk, D., Schofield, O., Falkowski, P.G., 2005. The role and evolution of superoxide dismutases in algae. Journal of Phycology, 41: 453-465.

Xie, R.C., Galer, S.J.G., Abouchami, W., Rijkenberg, M.J.A., de Baar, H.J.W., De Jong, J., Andreae, M.O., 2017. Non-Rayleigh control of upper-ocean Cd isotope fractionation in the western South Atlantic, Earth and Planetary Science Letters, 471: 94-103.

Zhao, Y., 2011. The carbon cycle and bioactive trace metals in the oceans: constraints from zinc isotopes. Dissertation, University of Bristol.

Zhao, Y., Vance, D., Abouchami, W., de Baar, H.J.W., 2014. Biogeochemical cycling of zinc and its isotopes in the Southern Ocean. Geochimica et Cosmochimica Acta, 125: 653-672.

Figure captions

full page: **Table 1.** Measured Fe and Zn uptake rates, cellular quotas, use efficiencies, and Zn isotope results ($\Delta^{66}Zn_{\text{biomass - medium}} = \delta^{66}Zn_{\text{biomass}} - \delta^{66}Zn_{\text{medium}}$).

two-column fitting image: **Fig. 1.** Comparison of surface area to biovolume (A/V) ratios for all phytoplankton cultured here to the ranges observed in natural communities as derived from MARine Ecosystem DATa (MAREDAT; Buitenhuis et al., 2013).

single-column fitting image: **Fig. 2.** Specific growth and metal uptake rates as a function of A/V ratios for all cultured diatoms and cyanobacteria.

single-column fitting image: **Fig. 3.** Cellular Fe and Zn quotas as a function of A/V ratios (A and B) and their interdependency (C) for all cultured diatoms and cyanobacteria.

single-column fitting image: **Fig. 4.** $\Delta^{66}Zn$ fractionation of cyanobacteria, which are variably well adapted to the applied nutrient and light conditions as a result of their different light harvesting strategies.

two-column fitting image: **Fig. 5.** Comparison of the Zn isotope fractionation upon uptake for all phytoplankton studied here, along with data from the literature. The red band indicates the range of $\Delta^{66}Zn$ values that could be explained simply by the presence of EDTA as a strong organic chelator in the culture medium, and published data for Zn isotope separation between Zn-EDTA and Zn^{2+} (Ban et al., 2002; Ding et al., 2010a; Ding et al., 2010b; Markovic et al., 2017).

Figure 1

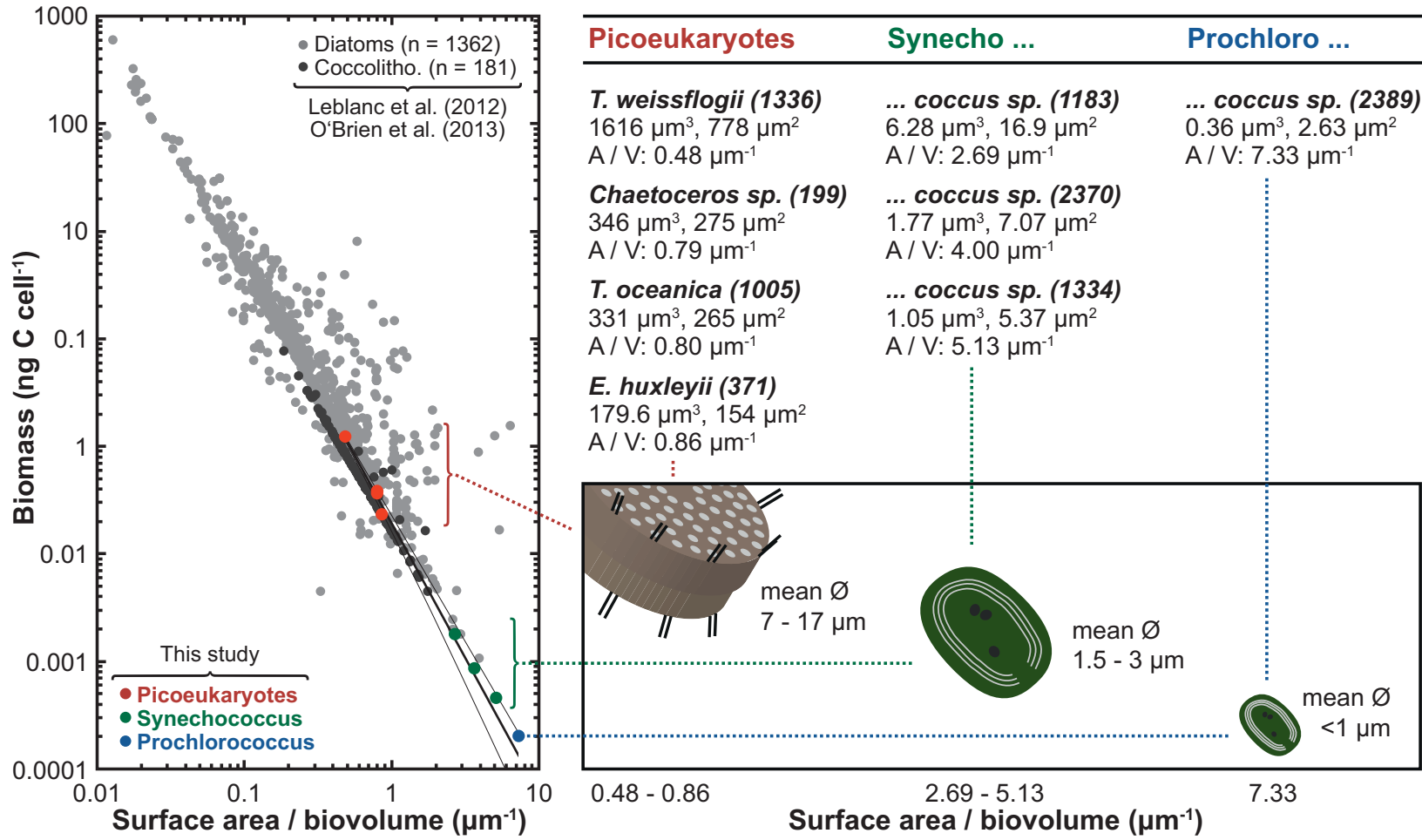
Biomass (ng C cell-1)
1000
100
10
0.1
1
0.01
0.001
0.0001
0.01
0.1
1
10
Surface area / biovolume (µm-1)
Diatoms (n = 1362)
Coccolitho. (n = 181)
Leblanc et al. (2012)
O'Brien et al. (2013)
This study
Picoeukaryotes
Synechococcus
Prochlorococcus
Picoeukaryotes
Synecho ...
Prochloro ...
T. weissflogii (1336)
1616 µm3, 778 µm2
A / V: 0.48 µm-1
Chaetoceros sp. (199)
346 µm3, 275 µm2
A / V: 0.79 µm-1
T. oceanica (1005)
331 µm3, 265 µm2
A / V: 0.80 µm-1
E. huxleyii (371)
179.6 µm3, 154 µm2
A / V: 0.86 µm-1
... coccus sp. (1183)
6.28 µm3, 16.9 µm2
A / V: 2.69 µm-1
... coccus sp. (2370)
1.77 µm3, 7.07 µm2
A / V: 4.00 µm-1
... coccus sp. (1334)
1.05 µm3, 5.37 µm2
A / V: 5.13 µm-1
... coccus sp. (2389)
0.36 µm3, 2.63 µm2
A / V: 7.33 µm-1
mean Ø
7 - 17 µm
mean Ø
1.5 - 3 µm
mean Ø
<1 µm
0.48 - 0.86
2.69 - 5.13
7.33
Surface area / biovolume (µm-1)

Figure 2

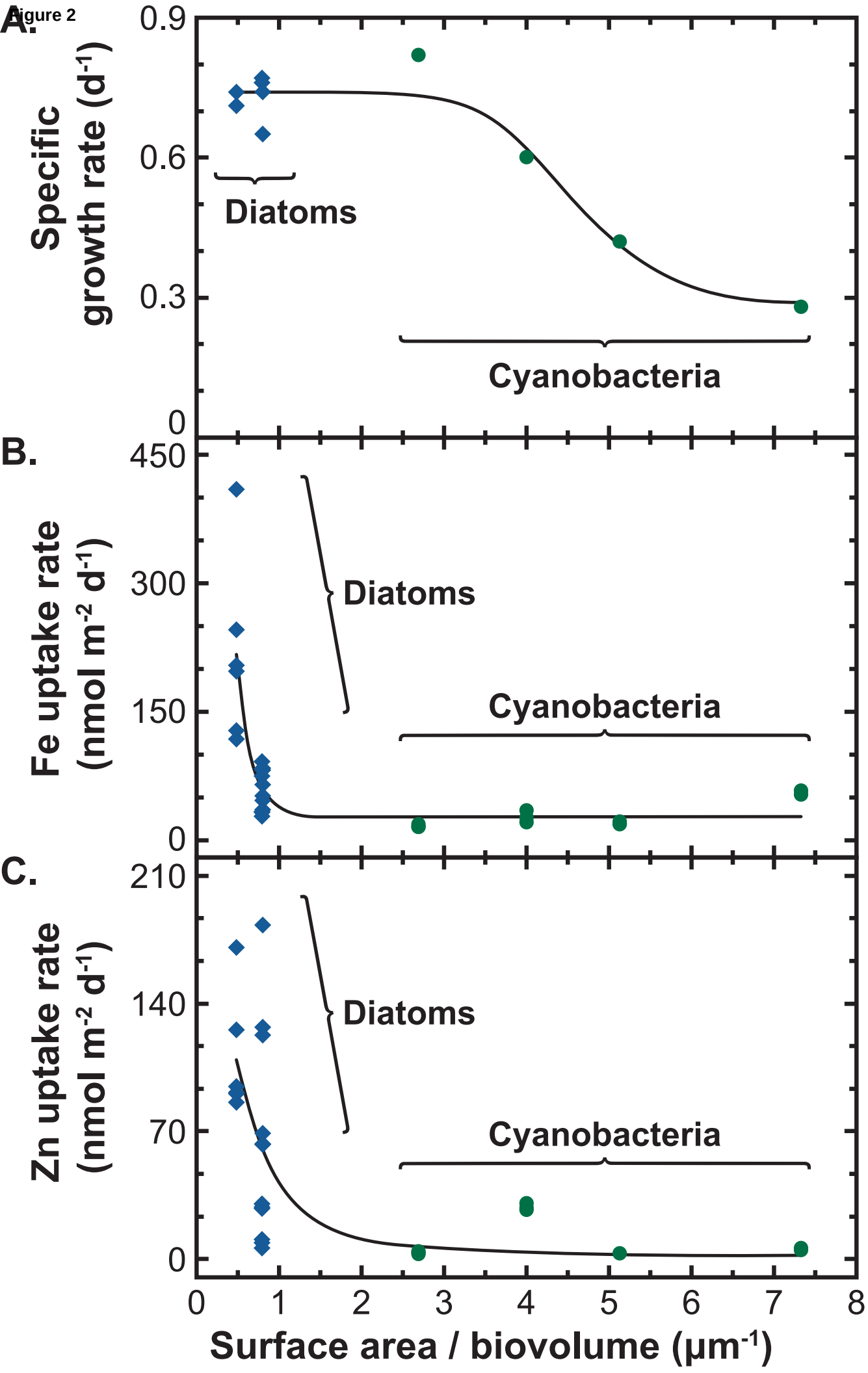
A.
Specific growth rate (d-1)
0.9
0.6
0.3
0
Diatoms
Cyanobacteria
B.
Fe uptake rate (nmol m-2 d-1)
450
300
150
0
Diatoms
Cyanobacteria
C.
Zn uptake rate (nmol m-2 d-1)
210
140
70
0
Diatoms
Cyanobacteria
0
1
2
3
4
5
6
7
8
Surface area / biovolume (µm-1)

Figure 3

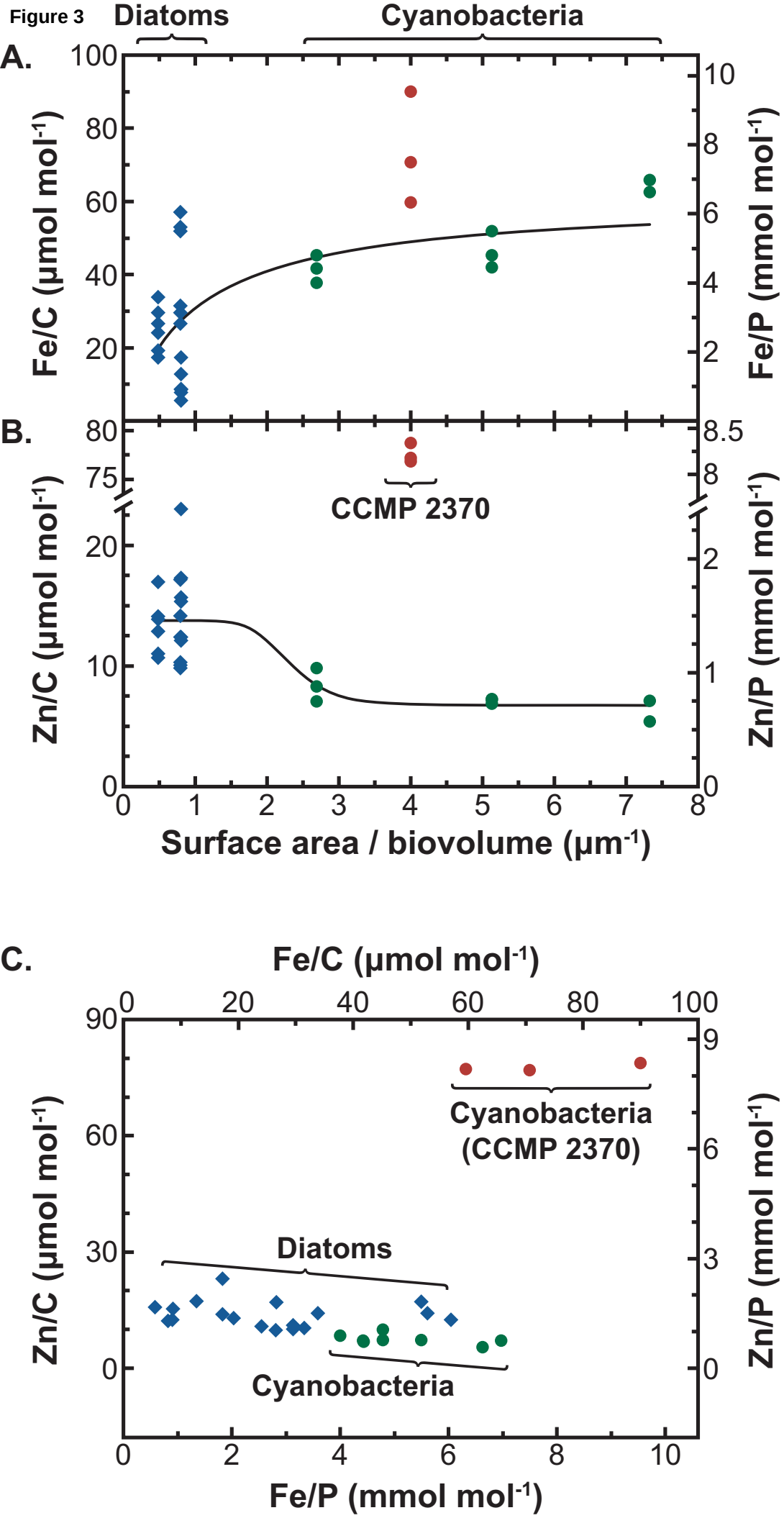
Diatoms
Cyanobacteria
A.
Fe/C (µmol mol-1)
Fe/P (mmol mol-1)
B.
Zn/C (µmol mol-1)
Zn/P (mmol mol-1)
CCMP 2370
Surface area / biovolume (µm-1)
C.
Fe/C (µmol mol-1)
Cyanobacteria
(CCMP 2370)
Diatoms
Cyanobacteria
Zn/C (µmol mol-1)
Zn/P (mmol mol-1)
Fe/P (mmol mol-1)

Figure 4

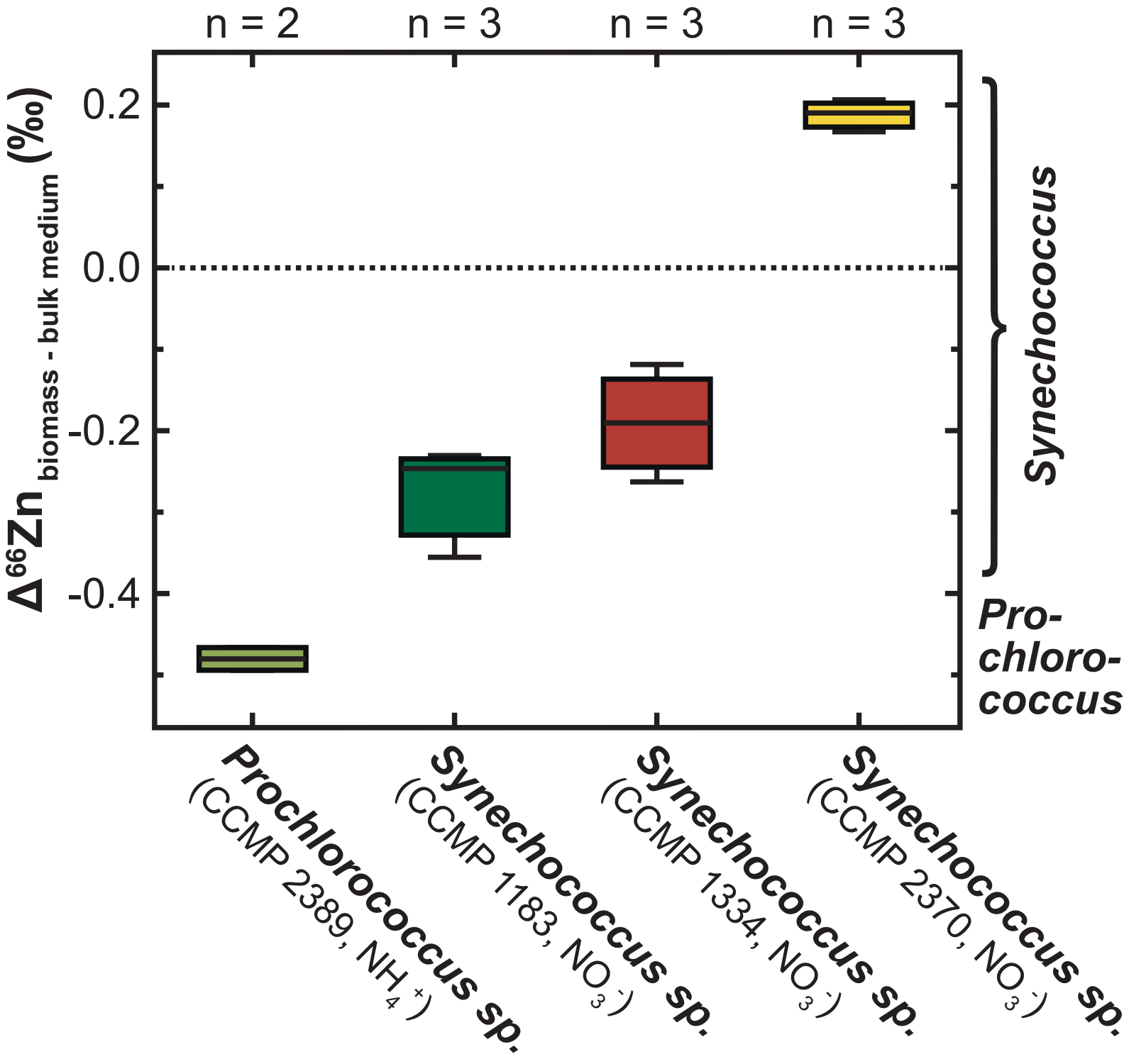
n = 2
n = 3
n = 3
n = 3
0.2
0.0
-0.2
-0.4
Δ66Zn biomass - bulk medium (‰)
Synechococcus
Pro-
chloro-
coccus
Prochlorococcus sp.
(CCMP 2389, NH4+)
Synechococcus sp.
(CCMP 1183, NO3-)
Synechococcus sp.
(CCMP 1334, NO3-)
Synechococcus sp.
(CCMP 2370, NO3-)

Figure 5

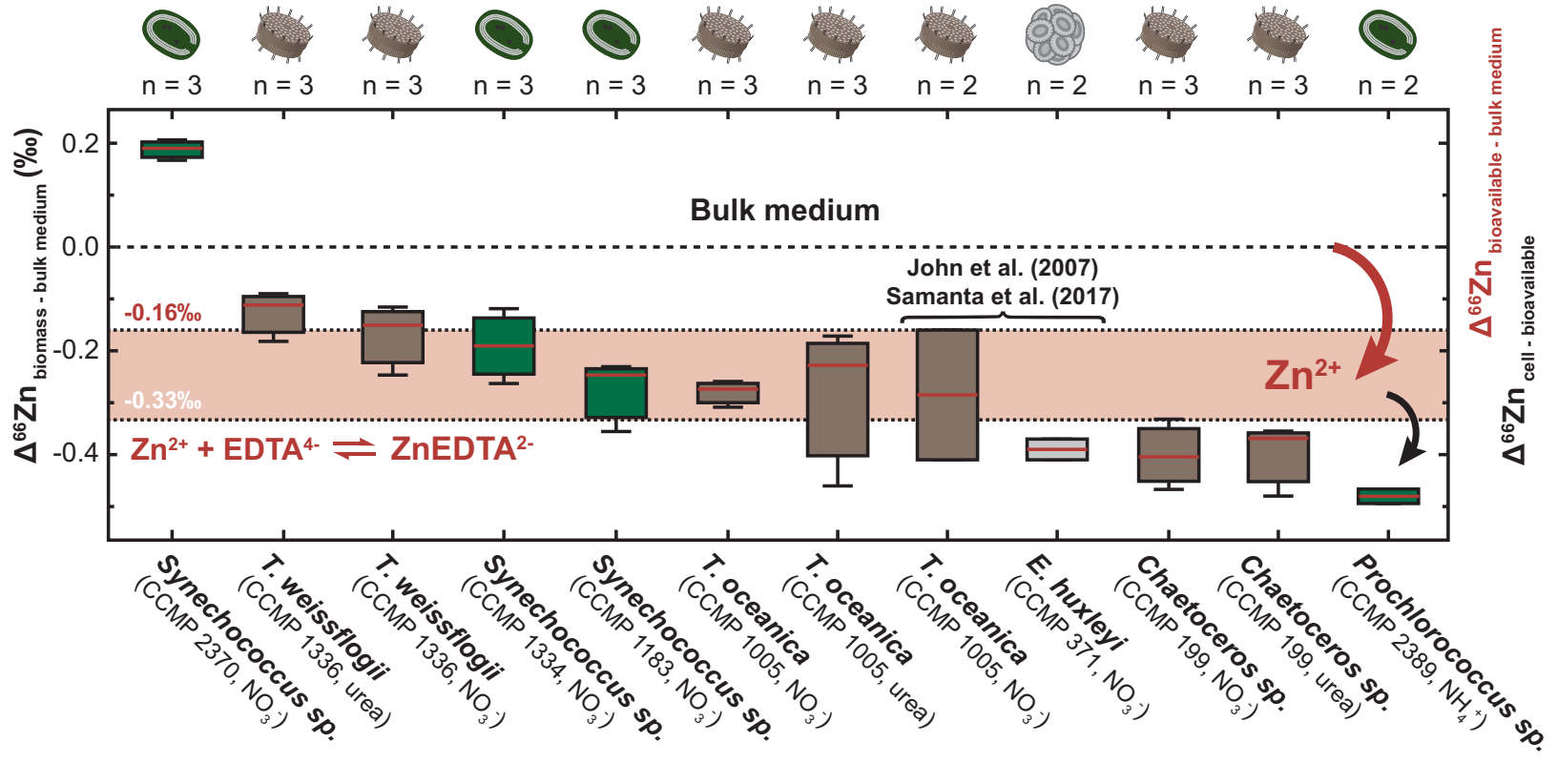
n = 3
n = 3
n = 3
n = 3
n = 3
n = 3
n = 3
n = 2
n = 2
n = 3
n = 3
n = 2
Δ66Zn biomass - bulk medium (‰)
0.2
0.0
-0.2
-0.4
Bulk medium
John et al. (2007)
Samanta et al. (2017)
-0.16‰
-0.33‰
Zn2+
Zn2+ + EDTA4- ⇌ ZnEDTA2-
Δ66Zn bioavailable - bulk medium
Δ66Zn cell - bioavailable
Synechococcus sp. (CCMP 2370, NO3-)
T. weissflogii (CCMP 1336, urea)
T. weissflogii (CCMP 1336, NO3-)
Synechococcus sp. (CCMP 1334, NO3-)
Synechococcus sp. (CCMP 1183, NO3-)
T. oceanica (CCMP 1005, NO3-)
T. oceanica (CCMP 1005, urea)
T. oceanica (CCMP 1005, NO3-)
E. huxleyi (CCMP 371, NO3-)
Chaetoceros sp. (CCMP 199, NO3-)
Chaetoceros sp. (CCMP 199, urea)
Prochlorococcus sp. (CCMP 2389, NH4+)

Figure S.1

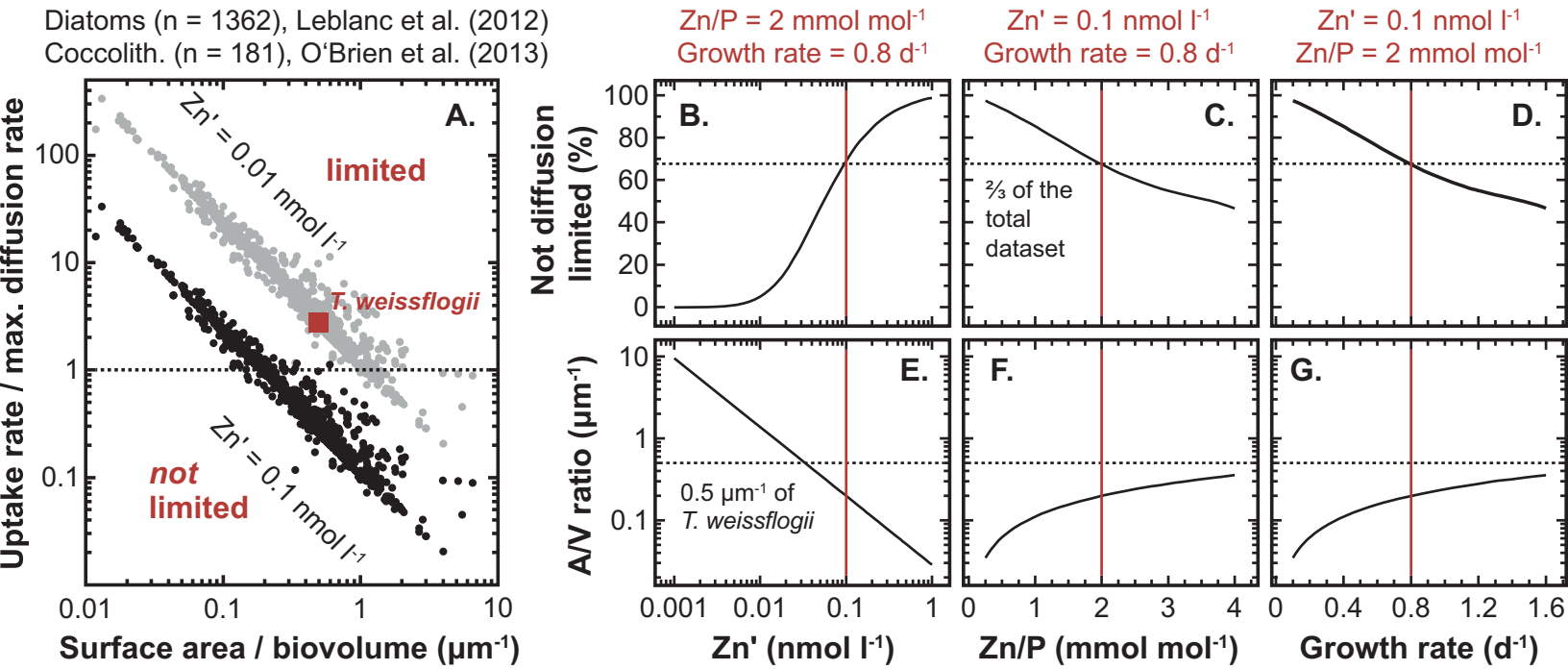
Diatoms (n = 1362), Leblanc et al. (2012)
Coccolith. (n = 181), O'Brien et al. (2013)
A.
limited
not limited
Zn' = 0.01 nmol l-1
Zn' = 0.1 nmol l-1
T. weissflogii
Uptake rate / max. diffusion rate
Surface area / biovolume (µm-1)
Zn/P = 2 mmol mol-1
Growth rate = 0.8 d-1
Zn' = 0.1 nmol l-1
Growth rate = 0.8 d-1
Zn' = 0.1 nmol l-1
Zn/P = 2 mmol mol-1
B.
C.
D.
⅔ of the total dataset
Not diffusion limited (%)
E.
F.
G.
0.5 µm-1 of T. weissflogii
A/V ratio (µm-1)
Zn' (nmol l-1)
Zn/P (mmol mol-1)
Growth rate (d-1)

Figure S.2

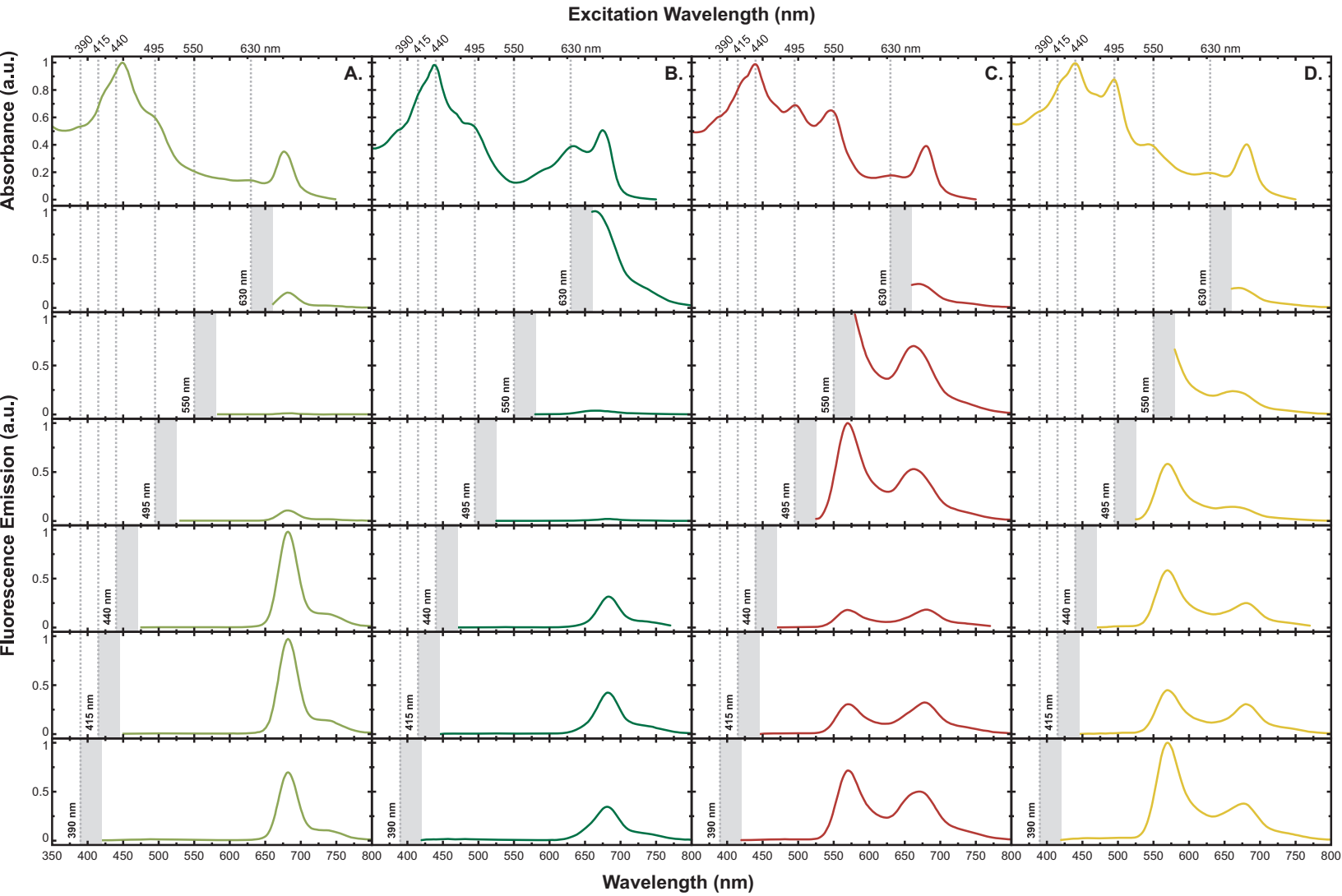
Excitation Wavelength (nm)
390
415
440
495
550
630 nm
A.
B.
C.
D.
Absorbance (a.u.)
Fluorescence Emission (a.u.)
630 nm
550 nm
495 nm
440 nm
415 nm
390 nm
Wavelength (nm)

Figure S.3

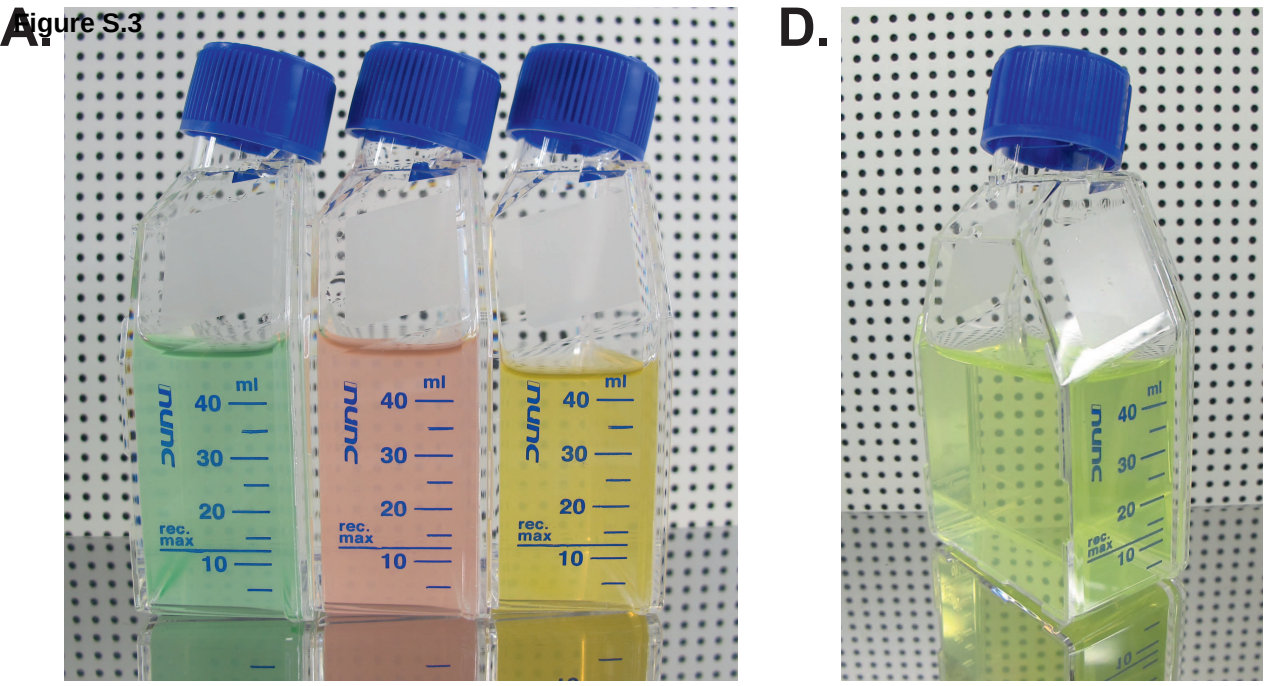
A.
D.

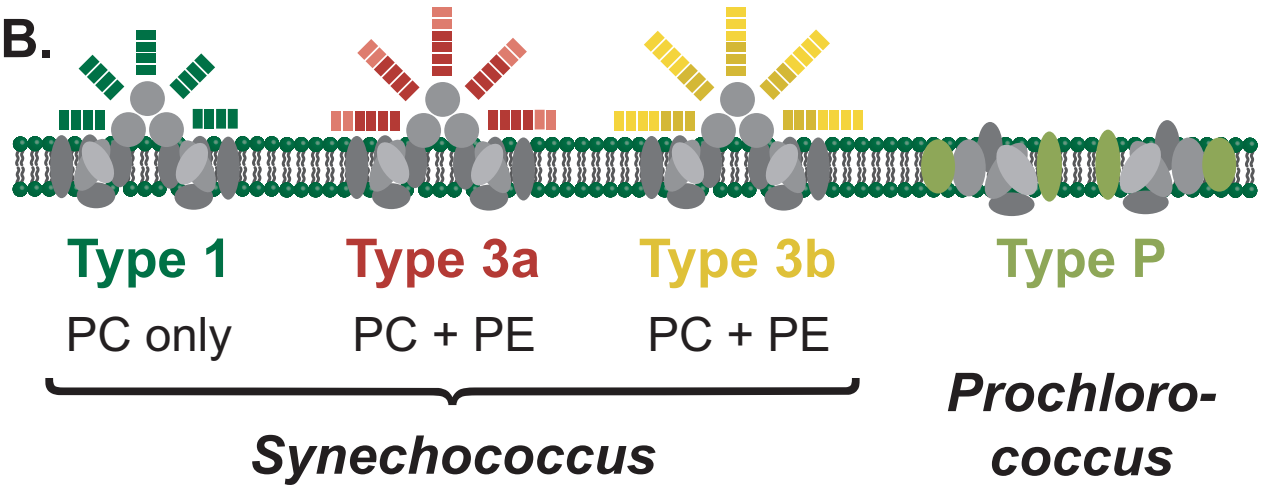
B.
Type 1
PC only
Type 3a
PC + PE
Type 3b
PC + PE
Type P
Synechococcus
Prochloro-
coccus

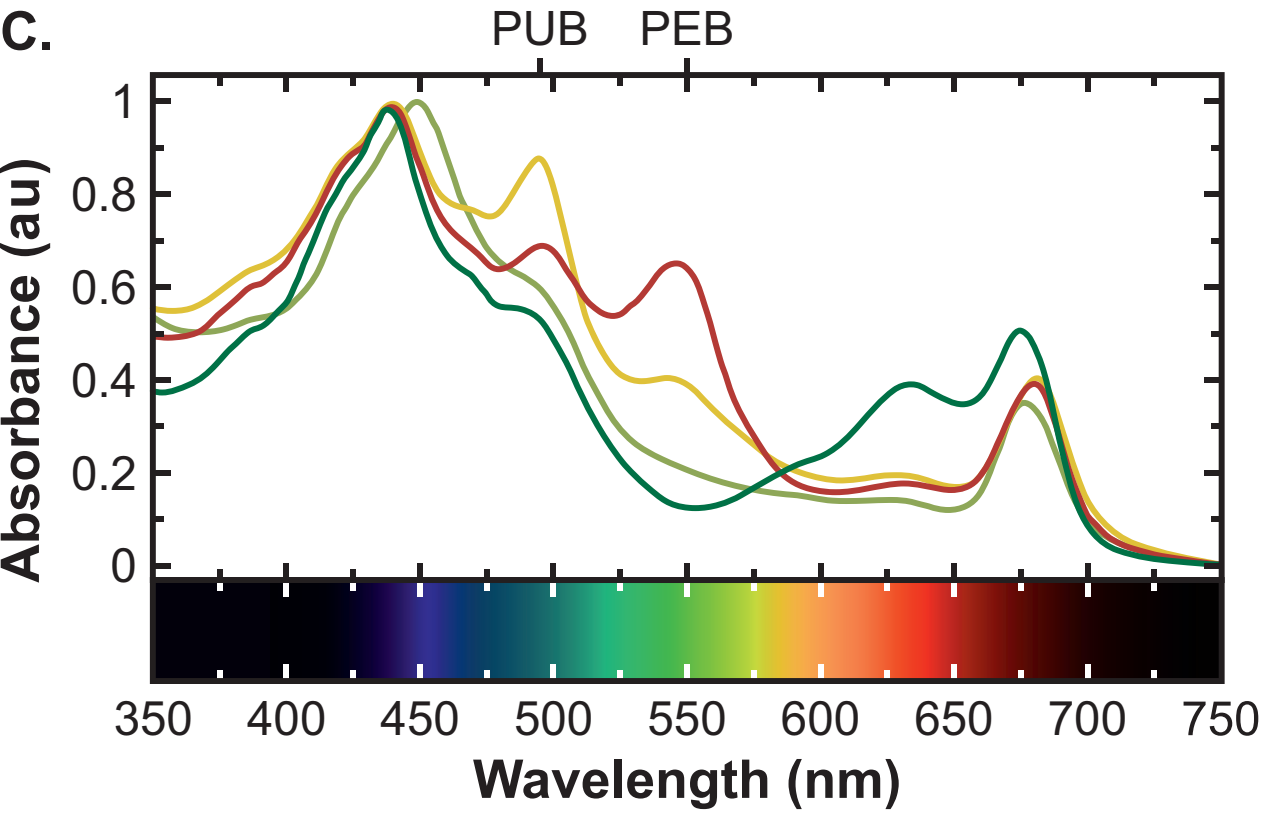
C.
PUB
PEB
Absorbance (au)
1
0.8
0.6
0.4
0.2
0
350
400
450
500
550
600
650
700
750
Wavelength (nm)

Figure S.4

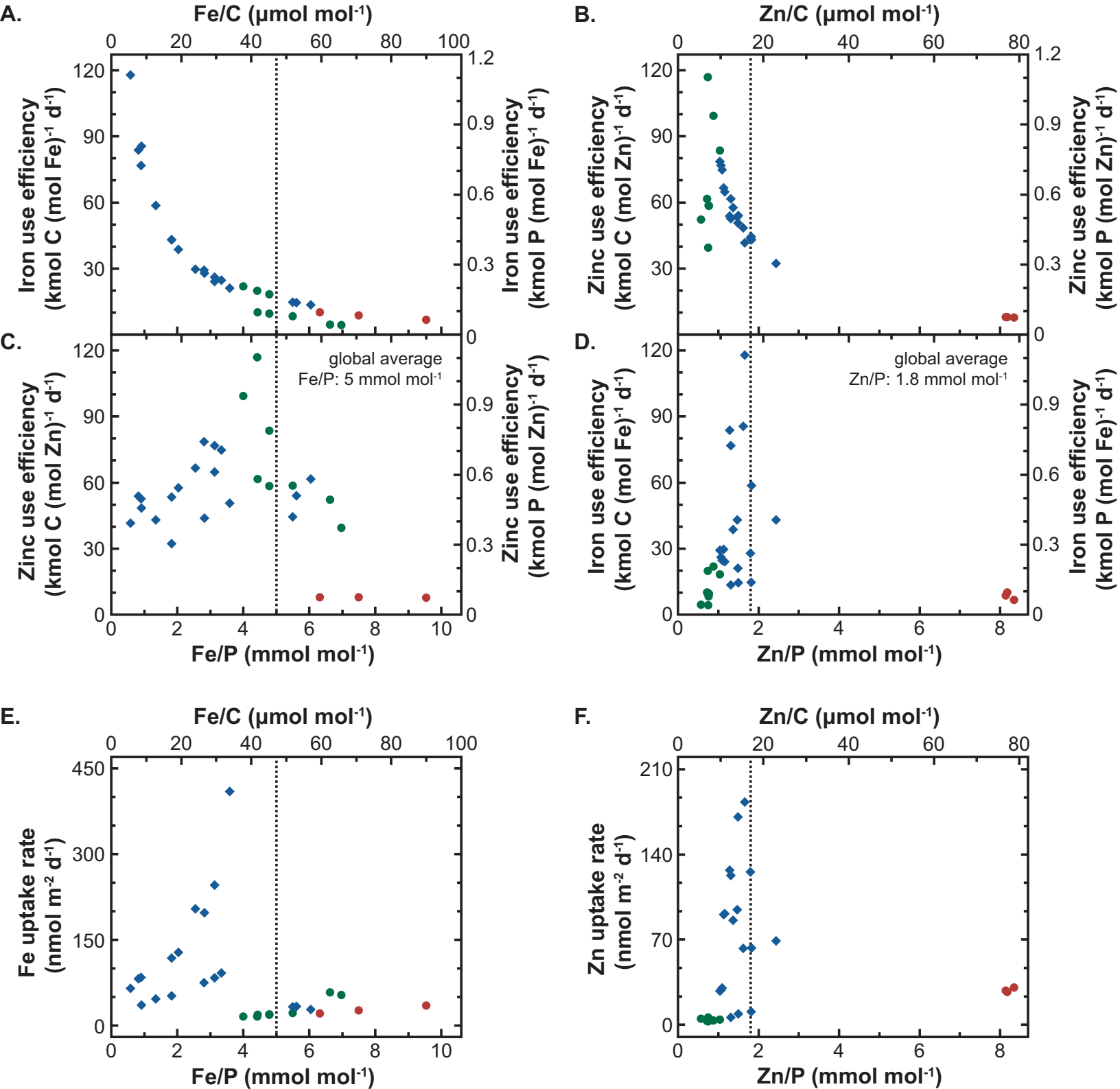
A.
Fe/C (μmol mol-1)
Iron use efficiency (kmol C (mol Fe)-1 d-1)
Iron use efficiency (kmol P (mol Fe)-1 d-1)
B.
Zn/C (μmol mol-1)
Zinc use efficiency (kmol C (mol Zn)-1 d-1)
Zinc use efficiency (kmol P (mol Zn)-1 d-1)
C.
global average
Fe/P: 5 mmol mol-1
Zinc use efficiency (kmol C (mol Zn)-1 d-1)
Zinc use efficiency (kmol P (mol Zn)-1 d-1)
Fe/P (mmol mol-1)
D.
global average
Zn/P: 1.8 mmol mol-1
Iron use efficiency (kmol C (mol Fe)-1 d-1)
Iron use efficiency (kmol P (mol Fe)-1 d-1)
Zn/P (mmol mol-1)
E.
Fe/C (μmol mol-1)
Fe uptake rate (nmol m-2 d-1)
Fe/P (mmol mol-1)
F.
Zn/C (μmol mol-1)
Zn uptake rate (nmol m-2 d-1)
Zn/P (mmol mol-1)

Table 1

Click here to download Table: table 1.eps

	Species / Strain	A/V	Shape	Growth conditions				Uptake rates **		Cell. quota		Use efficiency ‡		Diffusion ⁂		Zn isotopes	
				N source	Fe′	Zn′	μ*	Fe	Zn	Fe/P	Zn/P	IUE	ZUE	Fe′	Zn′	Δ^{66}Zn	2 σ
		μm^{-1}			pmol l^{-1} ...		d^{-1}	nmol m^{-2} d^{-1} ...		mmol mol^{-1} ...		kmol P (mol M)$^{-1}$ d^{-1} ...		%	%	‰	‰
Diatoms		0.48	cylinder	nitrate	367	109	0.74	246	91.2	3.13	1.16	0.226	0.610	7.31	13.8	-0.25	0.09
								204	90.5	2.55	1.13	0.278	0.627	6.06	13.7	-0.15	0.09
								409	170	3.58	1.49	0.198	0.476	12.2	25.7	-0.12	0.07
				urea	378	106	0.71	117	94.3	1.83	1.47	0.404	0.503	3.40	14.6	-0.11	0.07
	T. weissflogii							128	85.6	2.03	1.36	0.364	0.543	3.69	13.2	-0.18	0.11
	CCMP 1336							197	125	2.82	1.79	0.263	0.412	5.70	19.4	-0.09	0.07
		0.79	cylinder	nitrate	190	102	0.77	74.2	27.5	2.81	1.04	0.274	0.741	2.53	2.62	-0.47	0.06
								91.8	30.1	3.34	1.09	0.231	0.705	3.13	2.86	-0.33	0.06
								83.2	28.3	3.13	1.06	0.246	0.724	2.84	2.69	-0.40	0.07
				urea	178	100	0.76	33.3	8.89	5.61	1.50	0.135	0.508	1.21	0.86	-0.35	0.16
	Chaetoceros sp.							27.5	5.97	6.05	1.31	0.126	0.580	1.00	0.58	-0.37	0.18
	CCMP 199							32.0	10.6	5.49	1.82	0.138	0.418	1.16	1.02	-0.48	0.17
		0.80	cylinder	nitrate	190	102	0.74	35.3	62.5	0.92	1.62	0.807	0.455	1.18	5.82	-0.27	0.03
								46.2	63.0	1.34	1.83	0.551	0.404	1.54	5.87	-0.26	0.04
								51.6	68.9	1.83	2.44	0.405	0.304	1.72	6.42	-0.31	0.04
				urea	178	100	0.65	81.5	127	0.82	1.28	0.790	0.507	2.90	12.0	-0.17	0.06
	T. oceanica							83.7	122	0.90	1.31	0.724	0.495	2.98	11.6	-0.23	0.05
	CCMP 1005							64.5	183	0.59	1.66	1.111	0.392	2.30	17.3	-0.46	0.07
Cyanobacteria		2.69	prolate spheroid	nitrate	173	102	0.82	15.6	2.63	4.42	0.74	0.186	1.101	0.14	0.06	-0.36	0.11
	Synechococcus sp.							18.3	3.99	4.79	1.04	0.171	0.787	0.16	0.09	-0.25	0.08
	CCMP 1183							15.3	3.37	3.99	0.88	0.205	0.936	0.13	0.08	-0.23	0.09
	Synechococcus sp.	4.00	sphere	nitrate	173	102	0.60	34.7	30.3	9.54	8.34	0.063	0.072	0.19	0.43	0.21	0.03
	CCMP 2370							25.8	28.0	7.49	8.14	0.080	0.074	0.14	0.40	0.17	0.04
	(WH 8102)							20.8	26.9	6.32	8.18	0.095	0.073	0.12	0.38	0.19	0.05
	Synechococcus sp.	5.13	prolate spheroid	nitrate	173	102	0.42	18.8	3.07	4.44	0.72	0.095	0.579	0.09	0.04	-0.26	0.07
	CCMP 1334							19.6	3.13	4.78	0.76	0.088	0.549	0.10	0.04	-0.19	0.07
	(WH 7803)							21.2	2.93	5.50	0.76	0.076	0.551	0.11	0.04	-0.12	0.09
	Prochlorococcus sp.	7.33	prolate spheroid	ammonia	1198	139	0.28	53.2	5.75	6.96	0.75	0.040	0.372	0.03	0.04	-0.49	0.04
	CCMP 2389 (MED 4)							57.4	4.93	6.62	0.57	0.042	0.492	0.03	0.03	-0.47	0.04

* Including volumetric and handling errors we estimate the specific growth rate of replicates to have an uncertainty of less than ± 0.05 d^{-1}. ** Metal uptake rates are calculated after Sunda & Huntsman (1995, 1997), here normalized to the surface area of the cell. ‡ Metal use efficiencies are computed by dividing the specific growth rate by the cellular metal to phosphorus ratio, analogous to Raven (1990) and Sunda & Huntsman (2015). Iron (IUE) and zinc use efficiencies (ZUE) refer to the molar quantities of phosphorus build up per mole of metal, given in kmol P (mol Fe)$^{-1}$ d^{-1} and kmol P (mol Zn)$^{-1}$ d^{-1}, respectively. ⁂ Diffusion limitation has been estimated by comparing cellular metal uptake rates with maximum diffusion rates, following recipies introduced by Hudson & Morel (1990) and Sunda & Huntsman (1992). The tablulated results are given as a percentage of the cellular uptake rate over the maximum diffusion rate, calculated with diffusion rate constants of $9 \cdot 10^{-6}$ cm^2 s^{-1} (Hudson & Morel, 1990) and $6 \cdot 10^{-6}$ cm^2 s^{-1} (Sunda & Huntsman, 1992), for Fe′ and Zn′, respectively. This calculation is further described in Section S.2.